

CHAPTER 3

Result

3.1 Marker Horizons

A Total of 9 horizons were picked including the sea floor, from bottom to top they were named as H-1—H-9. Some of the horizons (H-1-H-3) were picked to show the initial fault trend and to establish their impact on igneous emplacement if there is any. Horizons from H-4—H-9 were picked to show their interaction with the igneous bodies and to see the structural variation created during igneous emplacement and sediment distribution with time and possible impact of igneous activity on sedimentation (Figs. 3.1, 3.2 and 3.3).

3.1.1 H-1

Horizon H-1 was picked the peak of high amplitude in 4.2 s TWT. It dips towards SW. It is a continuous horizon and easy to map until fault-A. It becomes discontinuous near igneous features.

3.1.2 H-2

Horizon H-2 was mapped on a trough of high amplitude around 3.7 s TWT. It generally dips towards west. It is continuous until the main fault A and is discontinuous near the igneous features.

3.1.3 H-3

Horizon was picked on a peak of high amplitude around 3.5 s TWT. It is approximately horizontal with small topographic change. It is continuous until the main fault A.

3.1.4 H-4

Horizon-4 was mapped on a peak of medium amplitude around 2.7 s TWT. It is continuous across in the entire basin except at igneous features. It is horizontal SW of main fault A, and is dipping towards NE beyond the fault.

3.1.5 H-5

Horizon-5 was mapped on peak of medium amplitude around 2.4 s TWT. It is a continuous, approximately horizontal on the SW side of the basin; it is truncated by the main fault A and is dipping towards NE beyond the fault.

3.1.6 H-6

Horizon-6 was mapped on a peak of low amplitude around 1.9 s TWT. It is continuous the SW side and is discontinuous at the NE side. It is discontinuous at and beyond igneous features.

3.1.7 H-7

Marker Horizon-7 was mapped on the peak of medium amplitude at 1.5 s TWT. It is continuous at the SW side and is discontinuous at and beyond the igneous features.

3.1.8 H-8

Marker horizon-8 was mapped on the trough of medium amplitude around 1.3 s TWT. It is a continuous horizon across almost the entire basin and is discontinuous at the igneous features present in the south.

3.1.9 H-9

This horizon was mapped on trough of high amplitude around 0.17 which marks the sea floor. It is continuous over the entire basin.

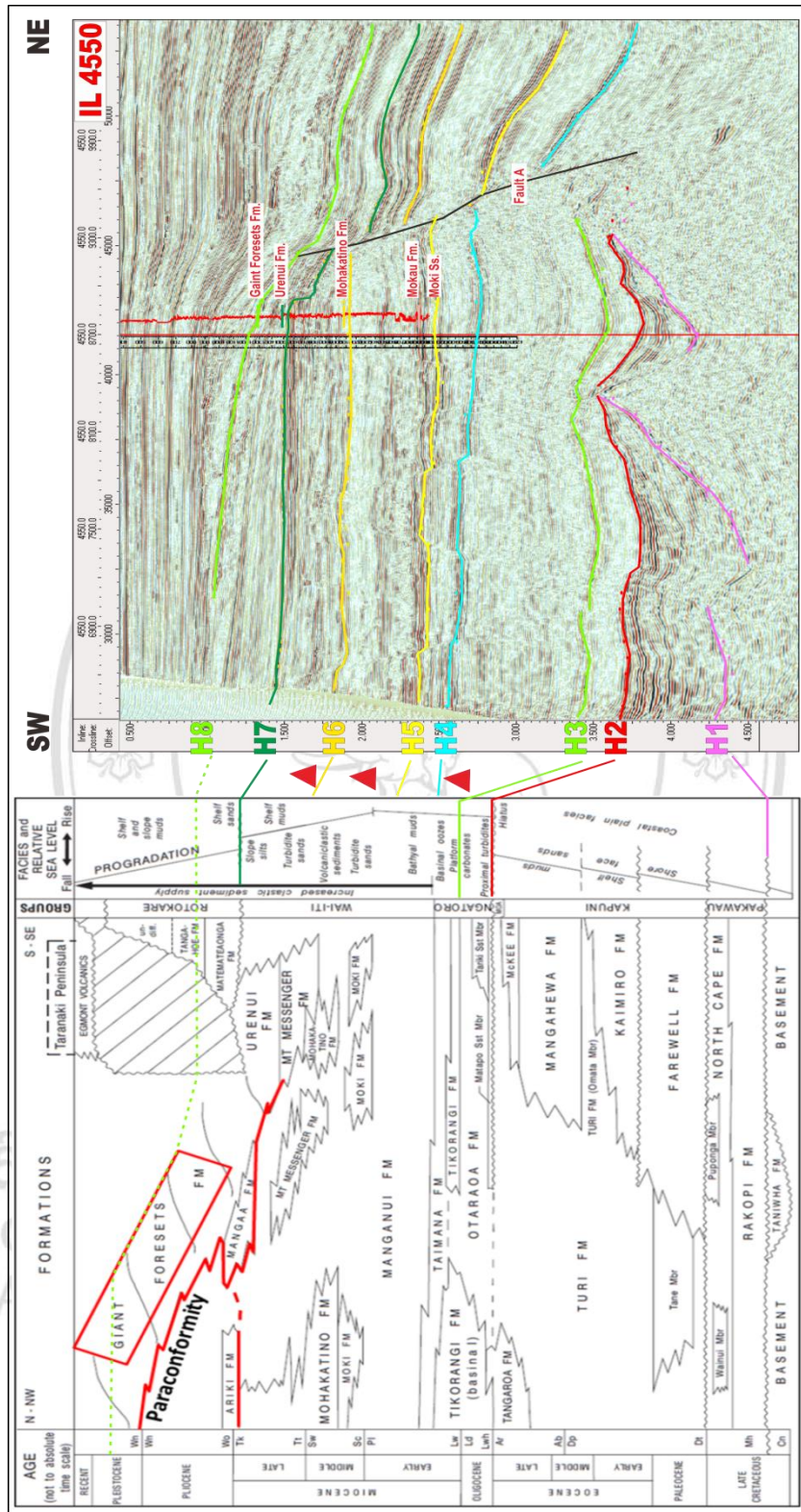


Figure 3.1 Regional stratigraphic column tied with the seismic showing the relative ages of the horizons

Table 3.1 The tectonic event from bottom to top along with well tops

Well tops	Relative age	Eq. Horizons	Tectonic event
		H-9	Extension, sagging
Giant Foresets	Plio-Pleistocene(3-1 Ma)	H-8	Extension, sagging
Urenui(1541)	L. Miocene-E. Pliocene(6-3)Ma	H-7	Extension, sagging
Mohakatino(2080)	L.Miocene(8-6)Ma	H-6	Extension, sagging
Mokau(2726)	L.Miocene(9-8)Ma	-	Second extension, sagging
Moki Ss(2948)	L.Miocene	H-5	Second extension sagging
	E. Miocene	H-4	Start of second extensional event
	Oligocene	H-3	Post rift
	Middle Eocene	H-2	Early post rift
*Basement	Late Cretaceous	H-1	Early extensional event(syn-rift)

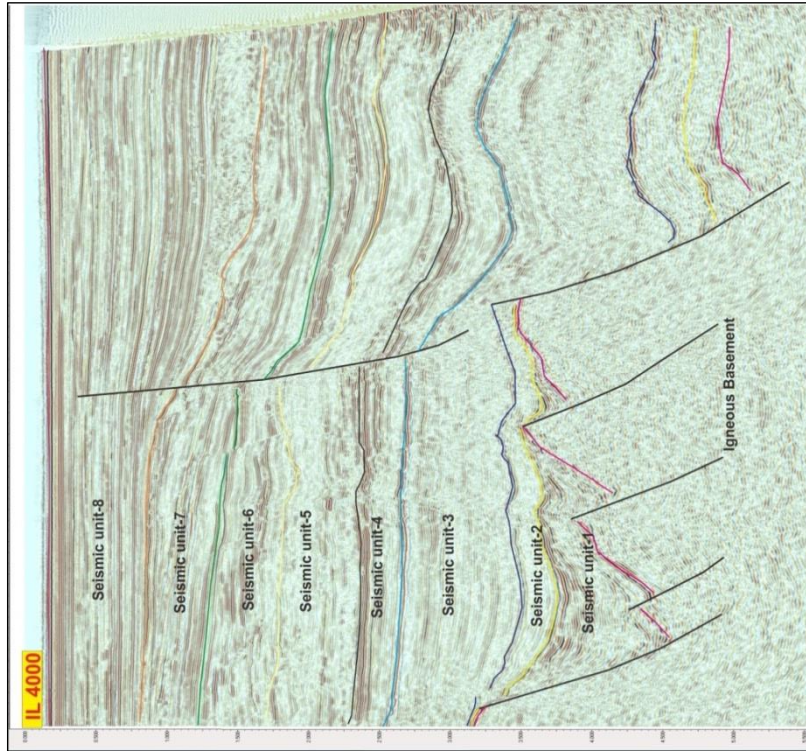


Figure 3.2 Showing interpreted seismic section

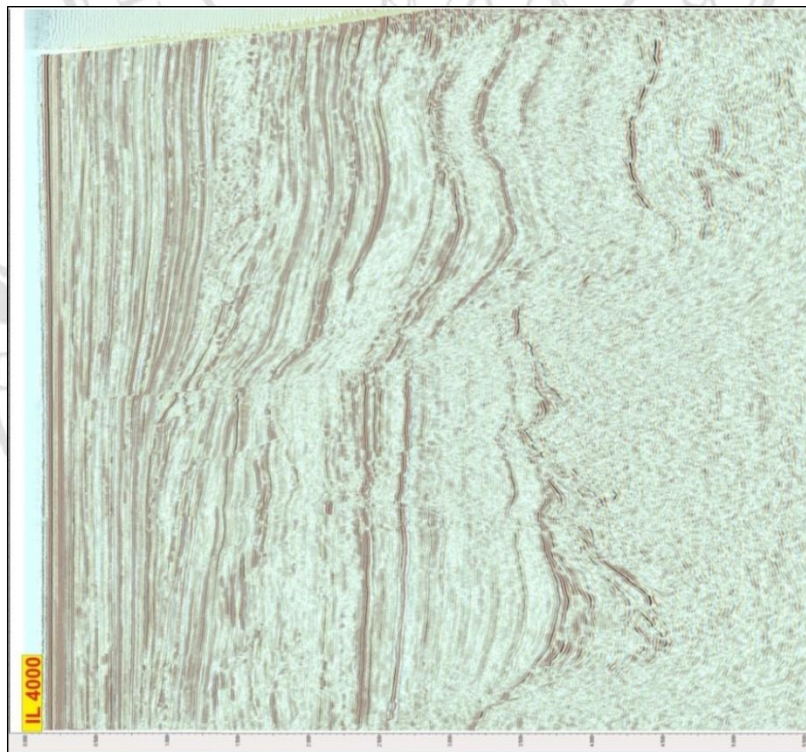


Figure 3.3 Showing uninterpreted seismic section

3.2 Structural style

Time structural maps of all the horizons were created (fig. 3.11) and the structural style of the H-1 horizon and H-4 horizon was compared. There are four major faults in the H-1 horizon. Rose diagrams of both the H-1 and H-4 horizons were created. Basement faults trend NNE-SSW while faults picked at H-4 – follow NE and ENE-WSW trends.

Basement faults show higher displacement ranging from 1 s TWT to 1.454 s TWT (about 1.3-1.9 km). Maximum displacement is seen along the main fault. The faults developed above horizon (H-4) shows NE and ENE-WSW orientations and have displacements in the range of 0.081 s TWT—0.242 s TWT (about 120-290m). The maximum displacement in the upper section faults is seen along the main fault which follows the same trend as the basement faults. The time structure maps and cross section of the H-1 horizon and H-4 horizon is given in Figures 3.7, 3.8, 3.9 and 3.10 respectively. The general fault trend of study area is shown on a series of time slices overlaid with coherency attribute in Figures 3.4, 3.5 and 3.6 respectively.

3.2.1 Time structure map of H-1 horizon

Time structure map of H-1 horizon shows structural highs located in between the faults and the lowest structural location is seen along the fault-A. Contour spacing is very narrow at the structural high and increases towards the structural lows (Figs. 3.7 and 3.11)

3.2.2 Time structure map of the H-2 horizon

Time structure map of the H-2 horizon shows that SW side of the study area has a structure high and contour spacing is of medium thickness. The structural low is located at the main fault for fault location see Fig. 3.7 and contour spacing is very narrow at the main fault (Fig. 3.11).

3.2.3 Time structure map of the H-3 horizon

Time structure map of the H-3 horizon shows that the structural high is located at the SW side of the study area and contour spacing is not very narrow and the lowest structure is located beyond the main fault and contour

spacing is very narrow near the main fault for fault location see Fig. 3.7 (Fig. 3.11).

3.2.4 Time structure map of the H-4 horizon

Time structure map of the H-4 horizon shows that structure high is located at the SW side and then there is structural low across the fault for fault location see Fig. 3.9. In the eastern part of the study area there is one structural high. In the middle of the study area there is structural low. Contour spacing is wide in the time structure map (Figs. 3.9 and 3.11).

3.2.5 Time structure map of the H-5 horizon

Time structure map of H-5 horizon shows a structural high on the NW side of this study area and structural low beyond the main fault for fault location see Fig. 3.9. Contour spacing is narrow near the fault and at the South of the area time structure map shows structural low (Fig. 3.11).

3.2.6 Time structure map of the H-6 horizon

Time structure map of the H-6 horizon shows the structural high at the SW side of the study area and structural low along the main fault, for fault location see Fig. 3.9. Contour spacing is wide in the NW half and closes in the SE half of the study area (Fig. 3.11).

3.2.7 Time structure map of the H-7 horizon

Time structure map of the H-7 horizon shows a structural high at the NW of the study area and structural low along the main fault, for fault location see Fig. 3.9. Contour spacing is wide in the NW and contour spacing is narrow towards the NE (Fig. 3.11).

3.2.8 Time structure map of the H-8 horizon

Time structure map of the H-8 horizon shows a structural high in the SW part of the study area and lowest structure is located along the main fault, for fault location see Fig. 3.9. The NE part of the study area shows a

structural low. Contour spacing is narrow in the NE part of the study area and wide in the SW (fig. 3.11).

3.2.9 Time structure map of the H-9 horizon

Horizon H-9 marks the sea floor and shows a gradual deepening towards the west (Fig. 3.11).



ลิขสิทธิ์มหาวิทยาลัยเชียงใหม่
Copyright© by Chiang Mai University
All rights reserved

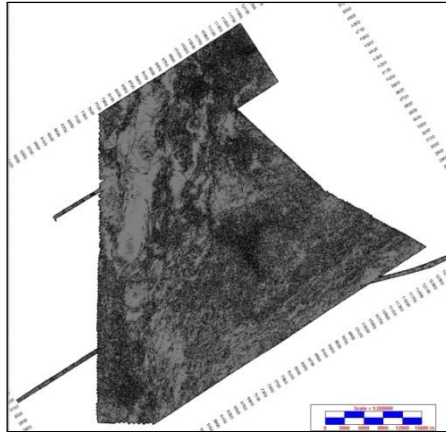


Figure 3.4 Showing time slice at 3.5 s TWT overlaid with coherency attribute

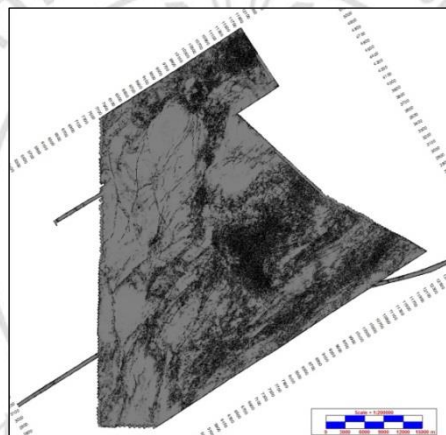


Figure 3.5 Showing time slice at 2.5 s TWT overlaid with coherency attribute

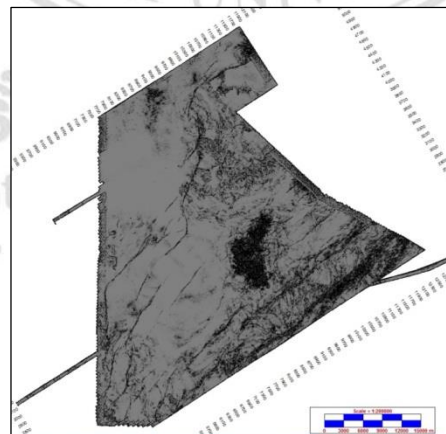


Figure 3.6 Showing time slice at 1.5 s TWT overlaid with the coherency

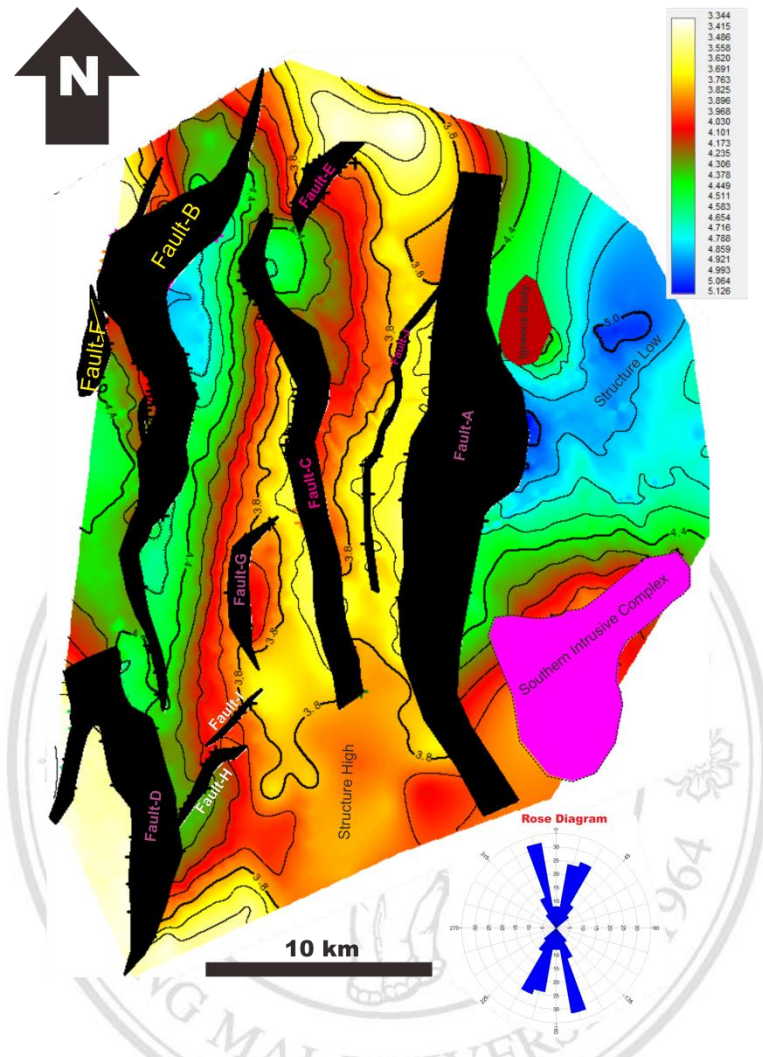


Figure 3.7 Time Structure map of the H-1 horizon

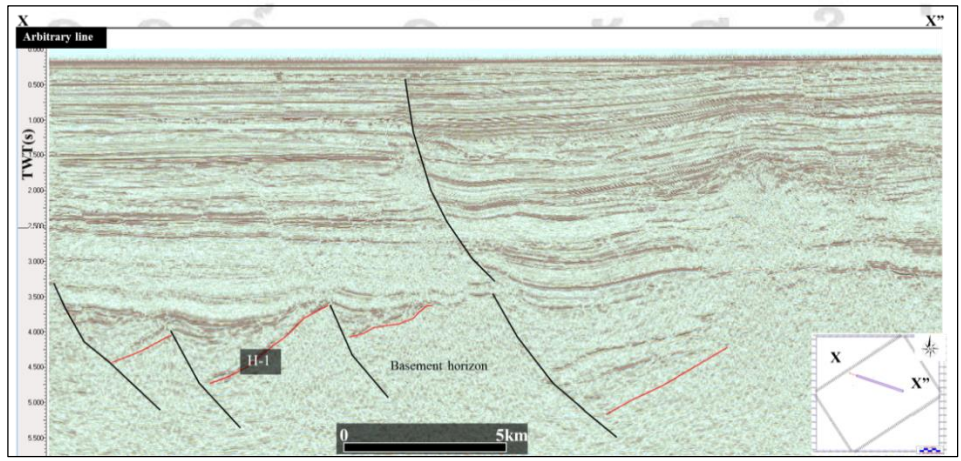


Figure 3.8 A cross section showing the H-1 horizon

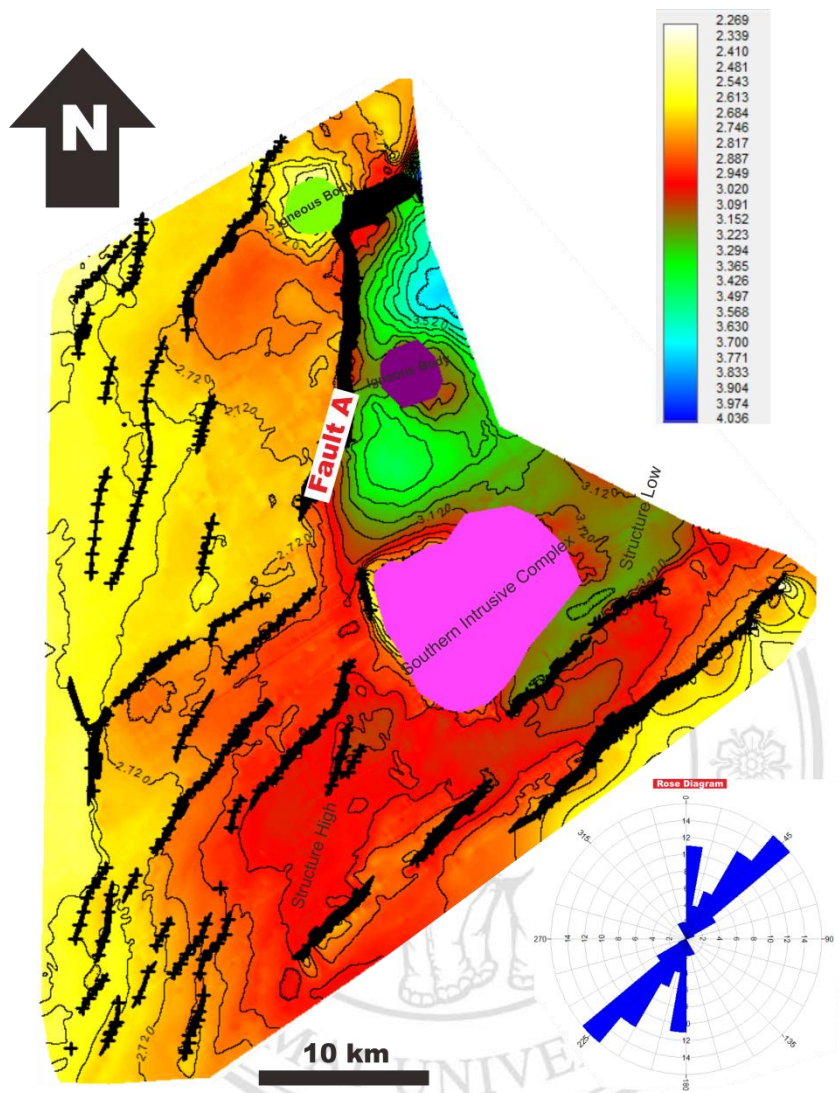


Figure 3.9 Time structure map of the H-4 horizon

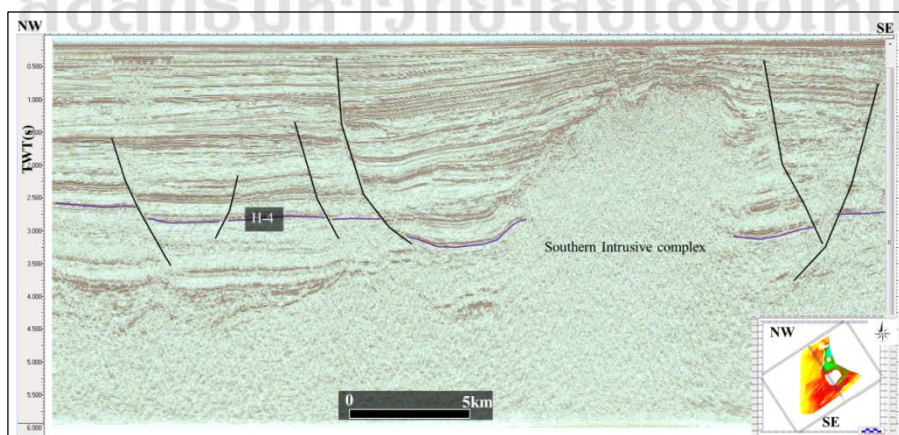


Figure 3.10 A cross section showing the H-4 horizon

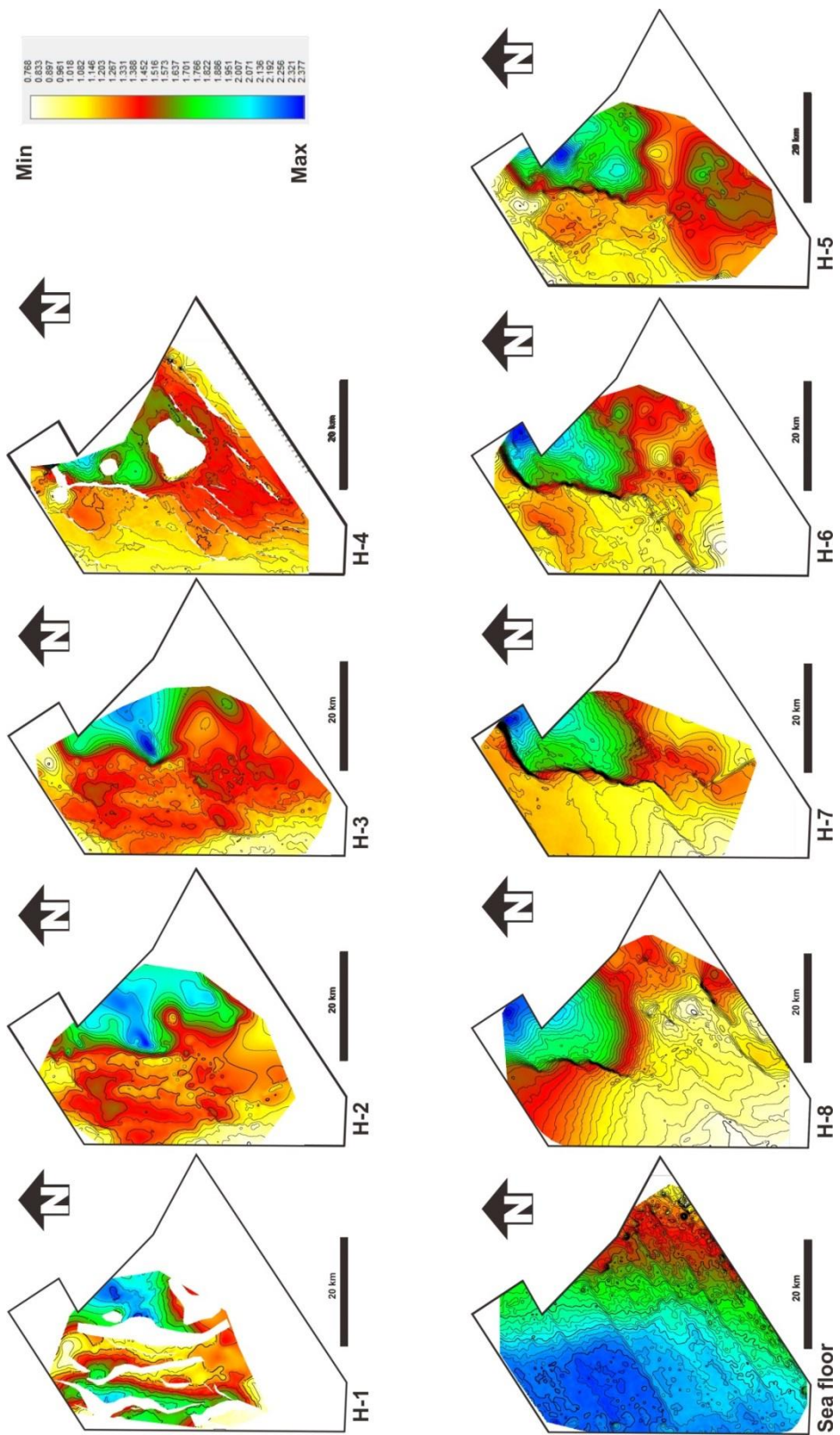
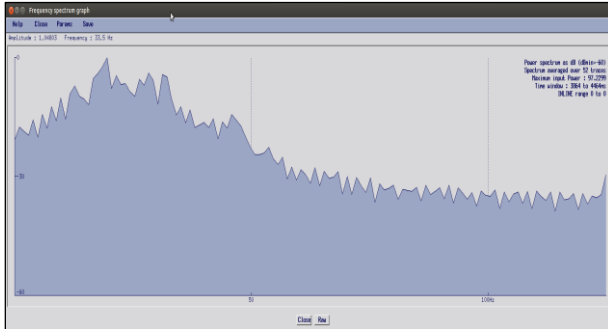


Figure 3.11 Shows the time structure maps of horizons H1-H9 (bottom to top)

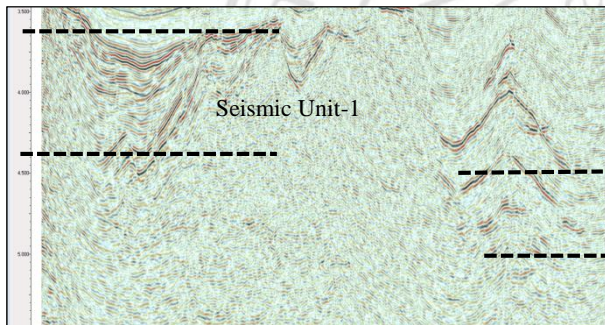
3.3 Seismic Units

A Total of eight seismic units were mapped from bottom to top and their seismic description are given in the ascending order from bottom to top in Fig. 3.3

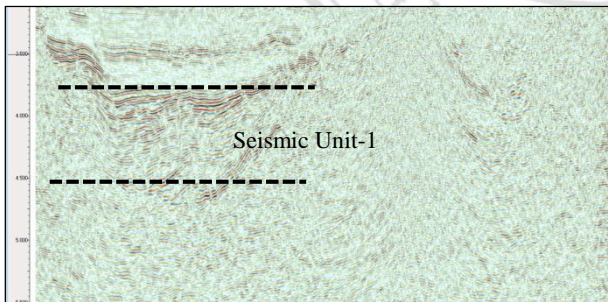
3.3.1 Seismic Unit 1



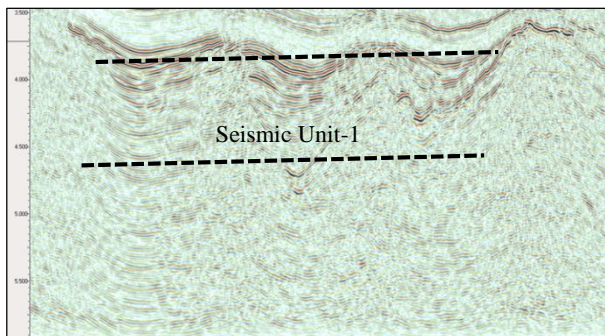
a. Frequency chart showing the dominant frequency in the seismic Unit-1.



b. IL 4120; XL 5700-10500, 3.5—5.0 s TWT. The line shows the internal reflection pattern and wedge shape geometry in the south-western part and chaotic pattern with mound shape in the northern part.

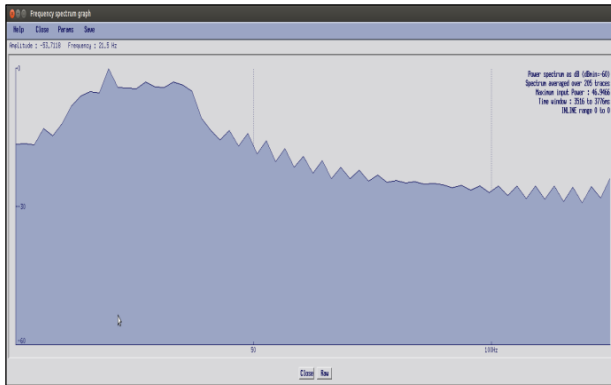


c. IL 5200; XL 5700—10500, 3.5—4.7 s TWT. Example of thickening of syn-rift strata of Unit-1 south-west wards. It shows the internal reflection pattern of parallel to sub-parallel and hummocky reflection pattern. It shows wedge shape geometry. At north-east side the strata are not imaged due to an igneous intrusion.

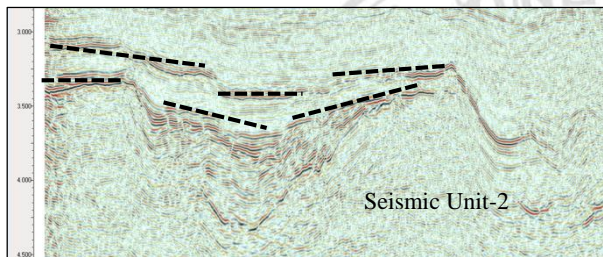


d. IL 4800; XL 6100—9900. 3.7—4.7 s TWT. It shows two normal fault-controlled wedge shape packages in Unit 1. Internal reflection pattern of parallel to sub-parallel and hummocky reflections.

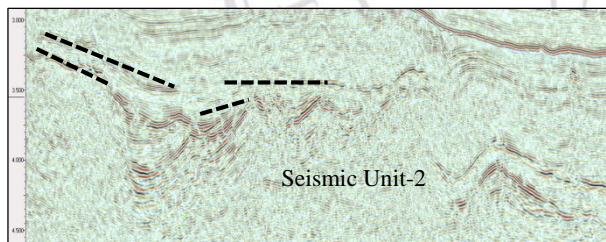
3.3.2 Seismic Unit 2



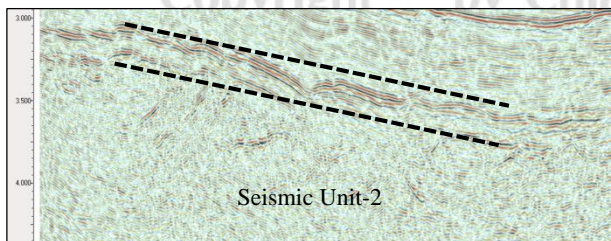
a. Frequency chart for Seismic unit-2. It shows dominant frequency of 28 Hz.



b. IL 5500; XL 7500—11100; 3.3—3.7 s TWT. It shows a very low amplitude reflection pattern, parallel to sub-parallel reflection pattern, thinning towards North. It has external shape of sheet which has at some places been displaced by faults

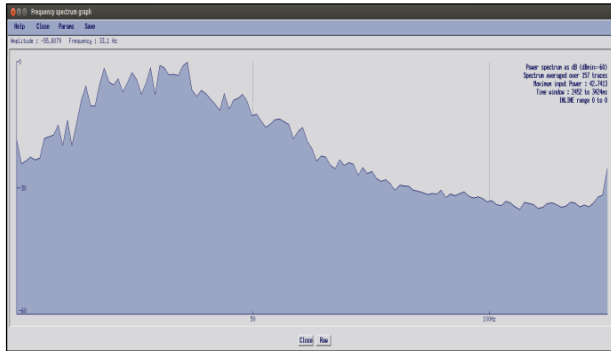


c. IL 3700; XL 5100—9800; 3.1—3.4 s TWT at proximal side of the basin and is mapped at 4.13 s TWT at distal side. It shows very low amplitude, parallel to sub-parallel and at some places deformed to chaotic reflection pattern. It shows the external shape of sheet drape/slope front fill.

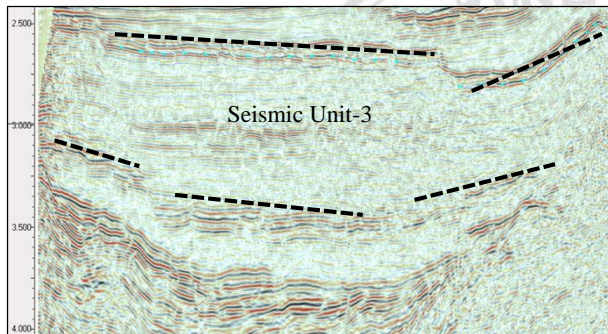


d. IL 2700; XL 3900—7700; 3—3.7 S TWT. It shows very low amplitude, parallel to sub-parallel reflection pattern. It has an external form of migrating wave.

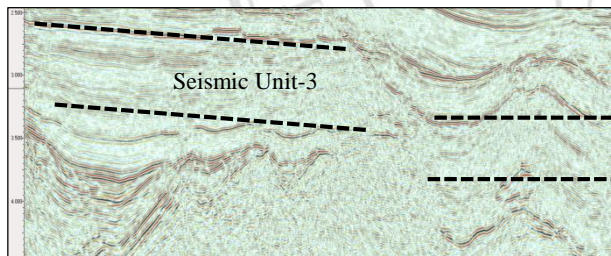
3.3.3 Seismic Unit 3



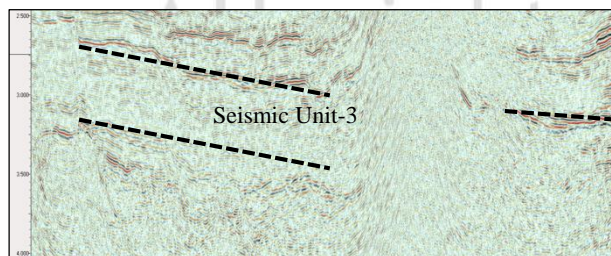
a. Frequency chart for the seismic unit-3 showing the dominant frequency.



b. IL 5250; XL 7200—11100; 2.5—3.4 s TWT. It shows very low amplitude reflection pattern, high frequency, parallel to sub-parallel reflection pattern. It has external form of sheet to sheet drape which has been displaced by faulting.

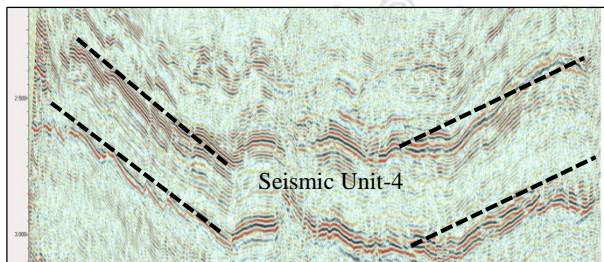
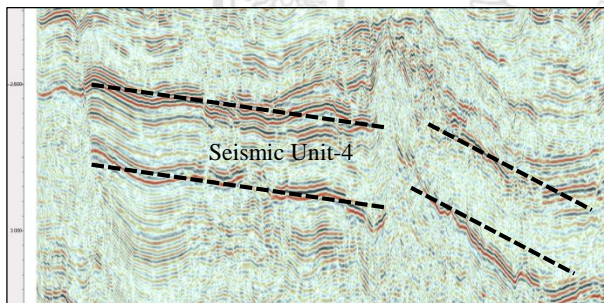
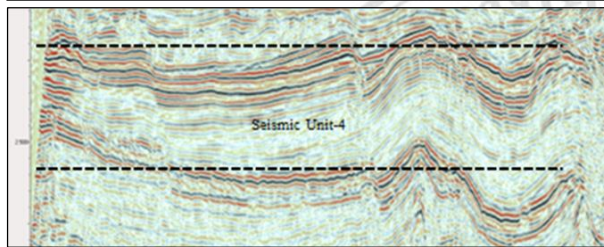
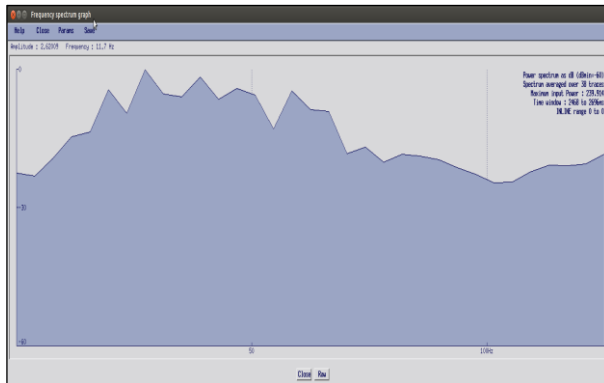


c. IL 4100; XL 5800—10800; 2.5—3.3 s TWT at SW side and 3.3—4.2 s TWT on NW side. It is a package of medium to low amplitude, medium to high frequency, parallel to sub-parallel internal reflection pattern. It has external form of sheet to sheet drape at SW side and mound shape on the NW side.



d. IL 3200; XL 4500—11100; 2.5—3.25 s TWT at SW side and 3.1—3.5 s TWT at NW side. It is a package of medium to low amplitude, high frequency, parallel to sub-parallel reflection pattern. It has external form of sheet and at places has been displaced by faulting. At NW side it not mappable.

3.3.4 Seismic Unit 4



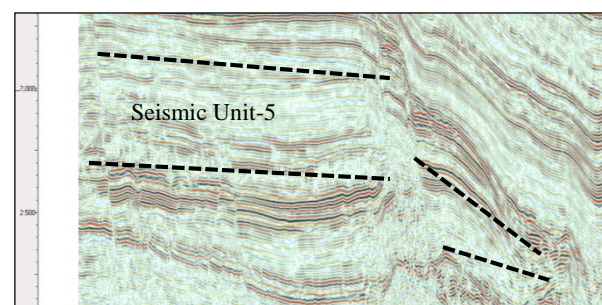
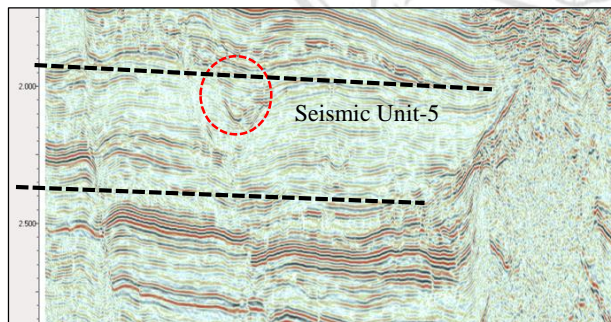
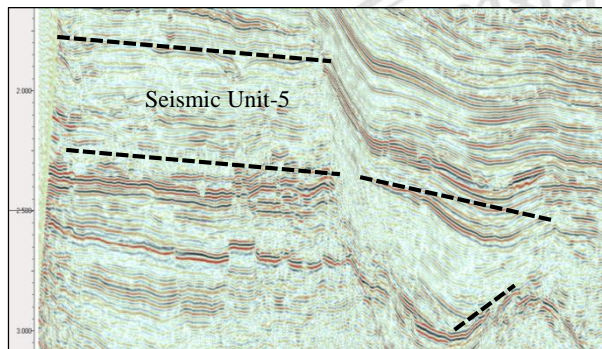
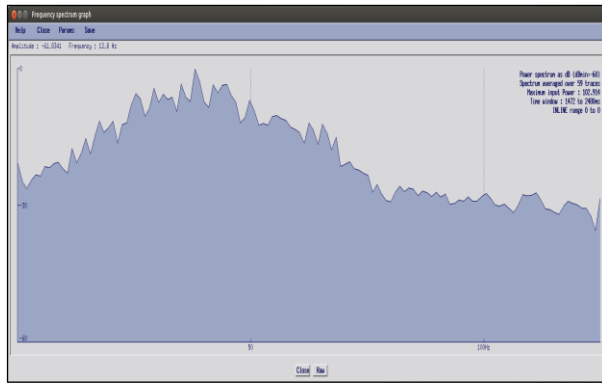
a. It shows the range of frequencies along with dominant frequency in the seismic unit-4.

b. IL 5400; XL 7500—11100, 2.2—2.6 s TWT. It is a package of medium to low amplitude. Its upper part has high amplitude while lower unit has low amplitude. It has parallel to sub-parallel internal reflection pattern. At SW side it has sheet drape external form and at North it has mound shape.

c. IL 3600; XL 5100—10500, It occurs between the time range of 2.5—2.7 s TWT at SW and between the time range of 2.6—3.2 s TWT at NW. At SW it is a package of medium to high amplitude and high frequency with parallel to wavy internal reflection pattern. It has been disrupted by the intrusion in the middle. At NW it has very low amplitude, reflection free zone. It has external form of sheet drape-mound.

d. IL 2600; XL 3900—11800. It occurs between the time window of 2.4—2.6 s TWT. It is a package of medium to low amplitude. It has high frequency. It has parallel internal reflection pattern at SW side and chaotic to reflection free at NE side. It has external form of wavy or broadly folded

3.3.5 Seismic Unit 5



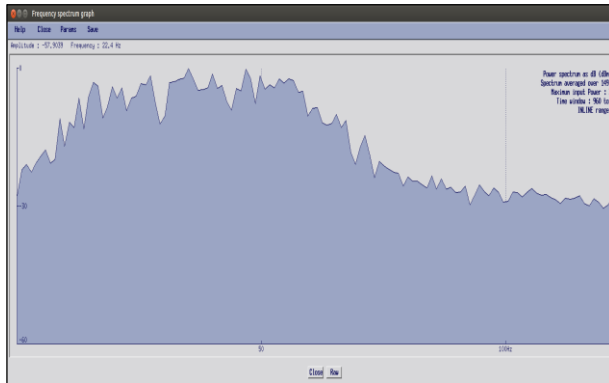
a. It shows the range of frequencies along with dominant frequency in the seismic unit-5.

b. IL 4100; XL 5700—10500; it occurs at the time window of 1.8—2.4 s TWT as South-westward and it is mapped at north-westward between time window of 2.4—2.7 s TWT. Towards the SW it is a package of medium to low amplitude, medium to high frequency with parallel to sub-parallel internal reflection pattern. Towards the NE it has very low amplitude and parallel-hummocky-lenticular internal reflection pattern. It has external form of sheet-basin-fill.

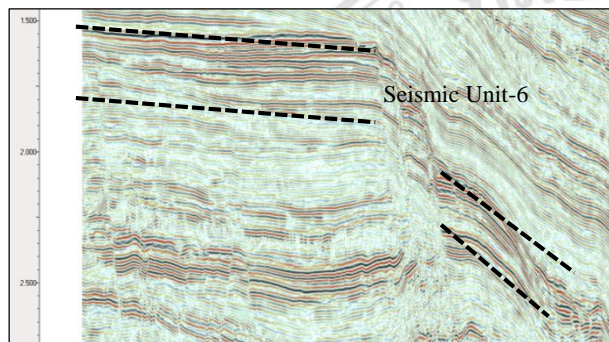
c. IL 3200; 5100—8700; at South west side it occurs at the depth of 1.92—2.4 s TWT. It has medium to low amplitude, medium to high frequency. It has parallel-sub-parallel internal reflection pattern. Complex fill can be seen in this package.

d. IL 5000; XL 6900—11700; it occurs at the time window of 1.9—2.4 at SW side and 2.4—2.7 at NE side. It is a package of medium to low amplitude. At the bottom of this unit it has chaotic reflection pattern. It has parallel to sub-parallel internal reflection pattern. It has external form of sheet at SW side and basin fill at NE side.

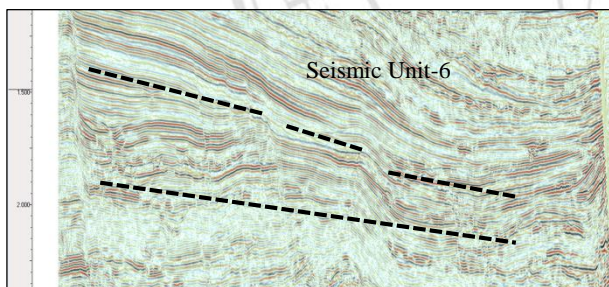
3.3.6 Seismic Unit 6



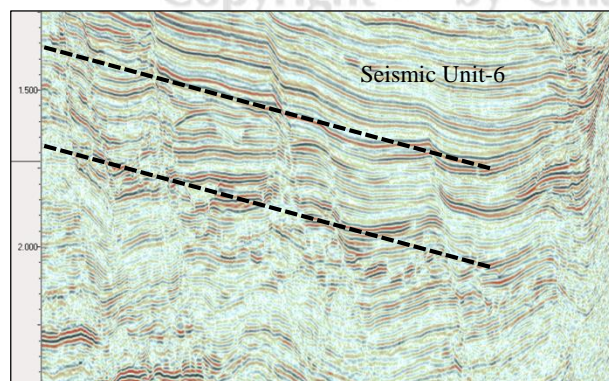
a. It shows the range of frequencies along with dominant frequency in the seismic unit-6.



b. IL 5000; XL 6900—11700; at SW side it occurs between the time window of 1.51—1.55 s TWT. On NE side it was mapped between the time windows of 2.1—2.4 S TWT. It is a package of medium to high amplitude, high frequency having a sub-parallel internal reflection pattern. It has sheet shape at SW side and basin fill shape at NE side.



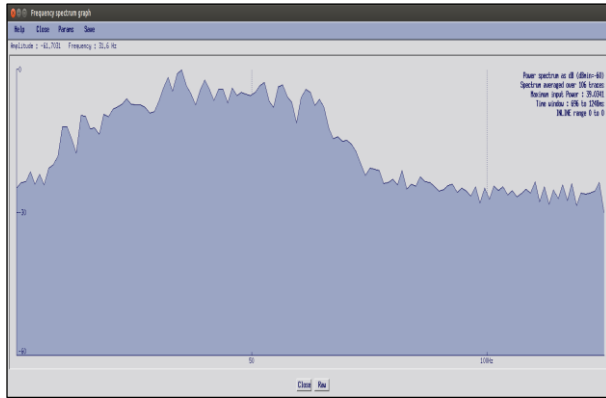
c. IL 3700; XL 5100—10500; it is located between the time window of 1.4—1.9 s TWT. It is a package of medium to high amplitude, high frequency. It has parallel to sub-parallel internal reflection pattern. It has external form of a slope front fill.



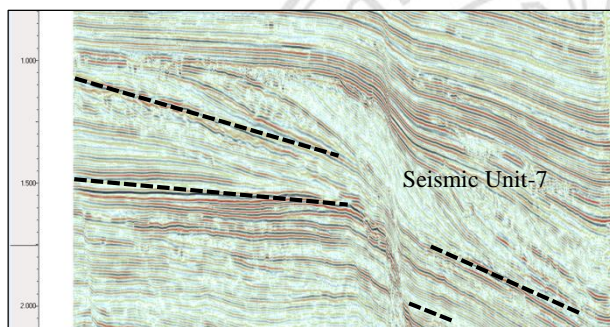
d. IL 3100; XL 4500—8100; it is occurred between the time window of 1.2—2.1 s TWT. It is a package of medium to high amplitude, high frequency. It has parallel to hummocky internal reflection pattern. It has external form of sheet drape.

ลิขสิทธิ์มหาวิทยาลัยเชียงใหม่
Copyright © by Chiang Mai University

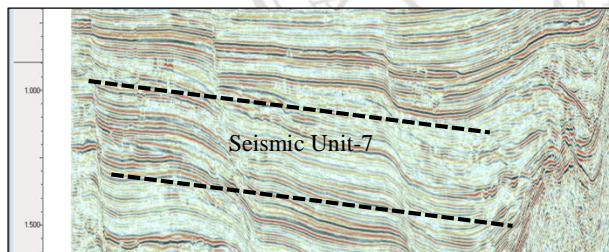
3.3.7 Seismic Unit 7



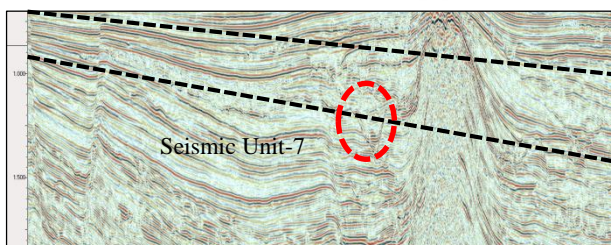
a. It shows the range of frequencies along with dominant frequency in the seismic unit-7.



b. IL 4900; XL 6900—11100. It is a package of medium to high amplitude, high frequency, and high continuity. It is located between the time window of 1—1.5 s TWT at SW side and 1.4—1.8 s TWT at North east ward. It has parallel to divergent internal reflection geometry. It makes a wedge shape external form at SW side and basin-fill shape at NE side.

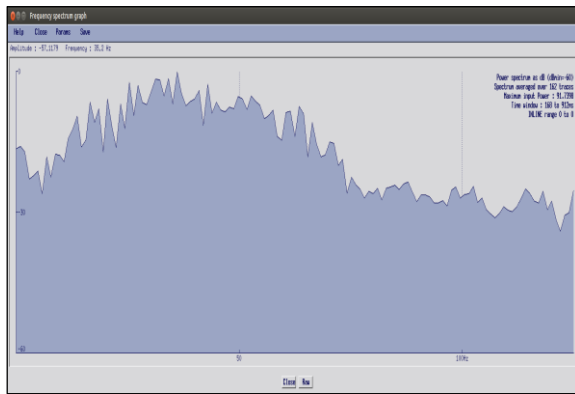


c. IL 3300; 5100—8700; It occurs between the time window of 0.8—1.4 s TWT. It is a package of medium to high amplitude, high frequency and high continuity. It has prograding clinoform internal reflection geometry. It has the external form of slope front fill.

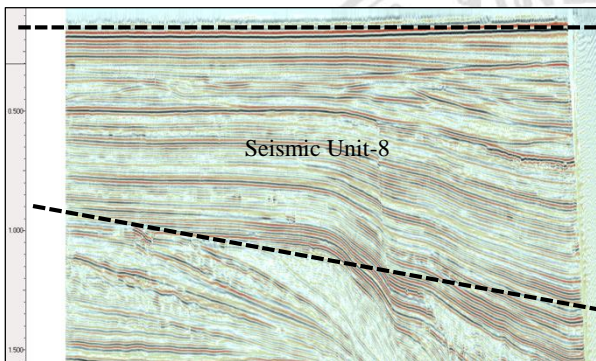


d. IL 2800; XL 4500—10500; it is mapped between the time window of 0.8—1.2 s TWT. It has medium to high amplitude, high frequency, and high continuity. It has a prograding clinoform internal reflection pattern. It has channel incision highlighted in red circle and the external form of slope front fill.

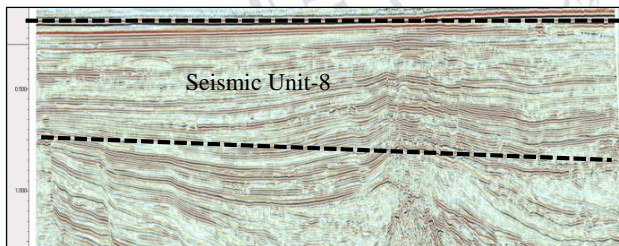
3.3.8 SeismicUnit 8



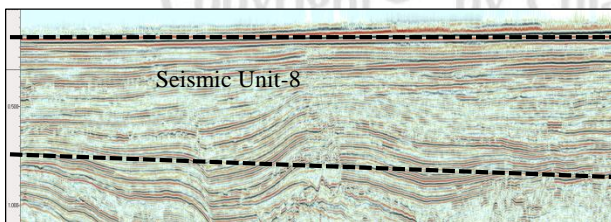
- a. It shows the range of frequencies along with dominant frequency in the seismic unit-8.



- b. IL 5000; XL 6900—11100; time window 0.2—1 s TWT. It is a seismic package of medium to high amplitude, high frequency. It extends along the whole length of the data. It has parallel to divergent internal reflection pattern at the lower unit and has lenticular reflection pattern in the upper unit. It has external form of basin fill for the lower unit and wedge shape for the upper unit.



- c. IL 3100; XL 4100—11100; time window 0.2—0.7 s TWT. It is a seismic package of medium to high amplitude, high frequency. In the lower part it has parallel to sub-parallel internal reflection pattern and at the upper part it has hummocky and complex fill internal reflection pattern. It has the external shape of migrating wave.



- d. IL 2500; XL 4500—11100; time window 0.2—0.7 s TWT. It has high amplitude and high frequency. It has parallel internal reflection pattern in its lower unit and wavy reflection pattern in its upper unit.

3.4 Isochrons of the units mapped

Isochrons were created for the horizons mapped from bottom to top (older to younger).

A total of 8 isochrons were created from bottom to top Fig. 3.12

3.4.1 Isochron between H-1—H-2

Isochron created between H-1 and H-2 shows a high thickness along the fault in the west and in the hangingwall of the main fault-A (Fig.3.7) there is also high thickness (Fig. 3.12).

3.4.2 Isochron between H-2—H-3

The isochron created between H-2 and H-3 shows that at the SW side of the study area there is a uniform thickness and the thickest part is located at the main fault for fault location see Fig. 3.9 (Fig. 3.12).

3.4.3 Isochron between H-3—H-4

Isochron between H-3 and H-4 shows high thickness at the SW side and the thickest part is located at the south. Near the igneous features it shows low thickness (Fig. 3.12).

3.4.4 Isochron between H-4—H-5

Isochron between H-4 and H-5 shows a fairly constant thickness in almost all the area mapped (Fig. 3.12).

3.4.5 Isochron between H-5—H-6

Isochron between H-5 and H-6 shows a gradual increase in thickness from the south to north in the area mapped and it shows the highest thickness along the major fault for fault location see Fig. 3.9 (Fig. 3.12)

3.4.6 Isochron between H-6—H-7

Isochron between H-6 and H-7 shows constant thickness along the both sides of the fault for fault location see Fig. 3.9 and shows thickest part along the fault for fault location see Fig. 3.9 (Fig. 3.12).

3.4.7 Isochron between H-7—H-8

Isochron between H-7 and H-8 shows the thinnest values at the south east of the study area and relatively thick values at the north-west of the area mapped (Fig. 3.12).

3.4.8 Isochron between H-8—H-9

Isochron between H-8 and H-9 shows that thickness gradually decreases passing towards the north (Fig. 3.12).

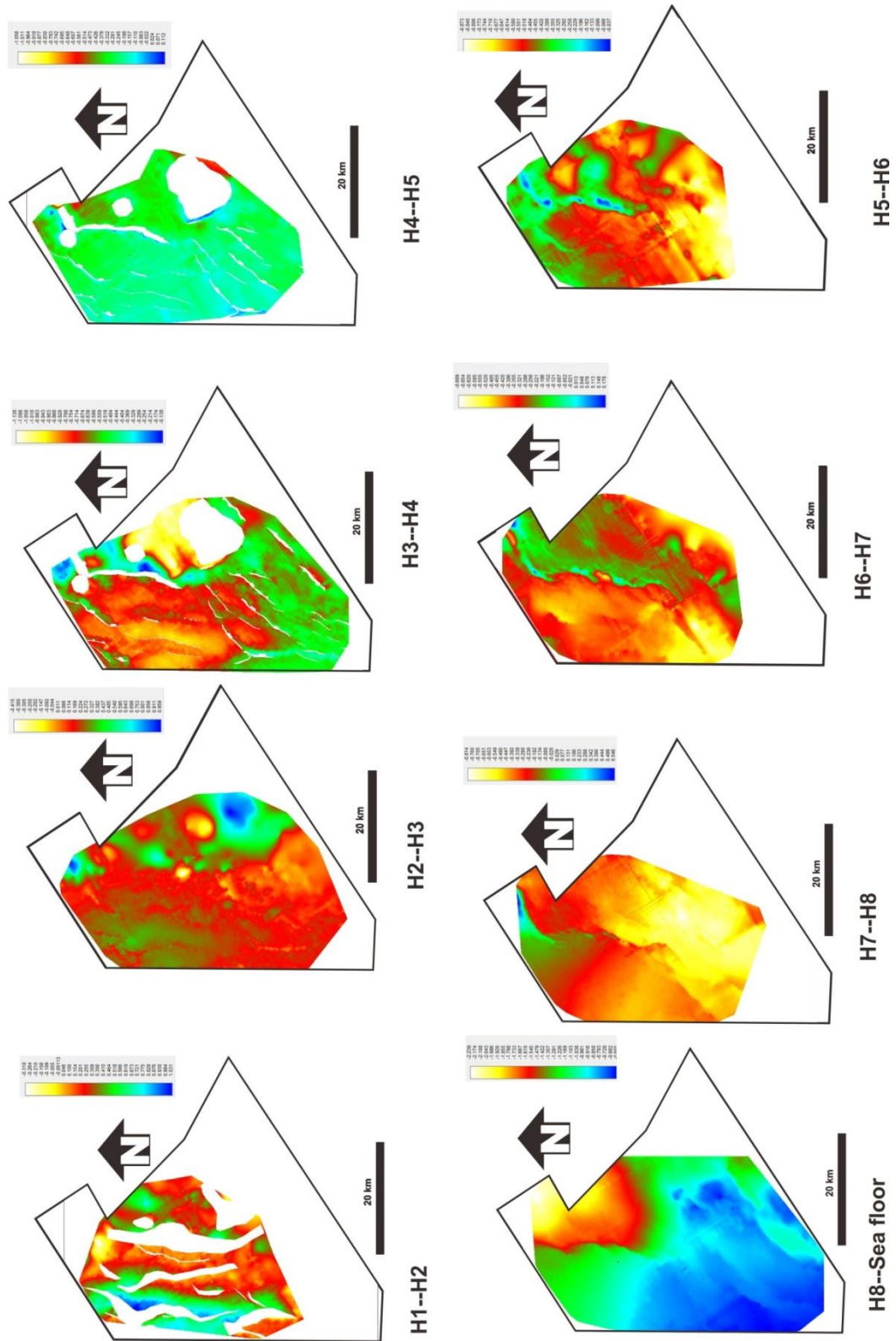


Figure 3.12 Isochrons of the horizons mapped from older to younger.

3.5 Volcanic Edifices

A total of 11 igneous bodies including extrusive and intrusive have been mapped, analysed and quantified. The igneous bodies trend from north to south and there is a very large intrusive complex at the south of the study area. Igneous bodies on seismic data are identified on the basis of high amplitude reflections, mound to convex upward, cone and dome shape which show varying degrees of flank dips. They can be confused with the shape of diapirs and salt diapirs. Salt diapirs are similar to volcanic edifices in having a reflection free zone, inside but unlike salt diapirs the volcanic edifice has parallel reflectors of high amplitude at their flanks due to the deposition of the volcanic clastics. In seismic data edifices look like a mound and can have height of up to 0.7 km and basal diameter of more than 5 km. Edifices have high amplitude reflectors at its top because as indicated by a decrease in Acoustic Impedance passing from soft rock (clastics) to hard rock (volcanics). At the flanks of the edifices the reflectors have steep dip which gradually decreases upon passing away from the edifices. They have mostly chaotic internal reflection pattern but along the flanks there are parallel dipping reflectors which can be due to the volcanoclastics eroding away from the edifices. If there is a substantial volcanic mountain then a flat top can be seen with the development of depression which represents the crater.

3.5.1 Conduit in seismic section

A conduit is the pathway for magma migration to the top. Conduits are vertical to sub-vertical features and that is why seismic techniques cannot image them well or at all. In the study area there is one possible example of conduit below volcanic edifice. The reflectors are discontinuous in a narrow zone. Velocity pull-ups can be observed, but they may be related to the overlying edifice rather than the conduit (Fig. 3.13).

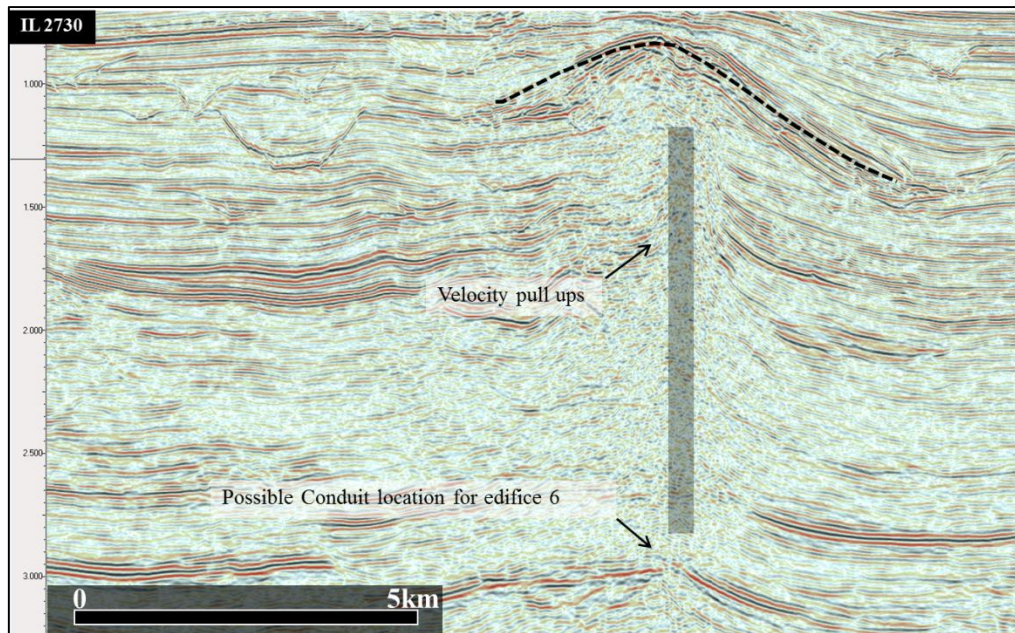


Figure 3.13 Possible conduit location in the seismic section.

3.5.2 Detailed interpretation of volcanic edifices

There are many igneous intrusions in the North Taranaki graben and the igneous activity in the North Taranaki graben began around ~16 Ma (Giba et al., 2010). These igneous features were mapped and their internal architecture was defined. The three dimensional geometry of the igneous intrusions were constrained and a measurement of the shapes of the edifices was undertaken. Igneous intrusions interact with the sediments and they can cause the change in local topography and even at some places they can trigger earthquakes. The aim of this study was to establish the distribution of the volcanic edifices in the study area (North Taranaki Graben) as well as their emplacement style, intensity, internal architecture and impact on sedimentation. Seismic facies analysis of the igneous intrusions was performed and their growth was mapped out.

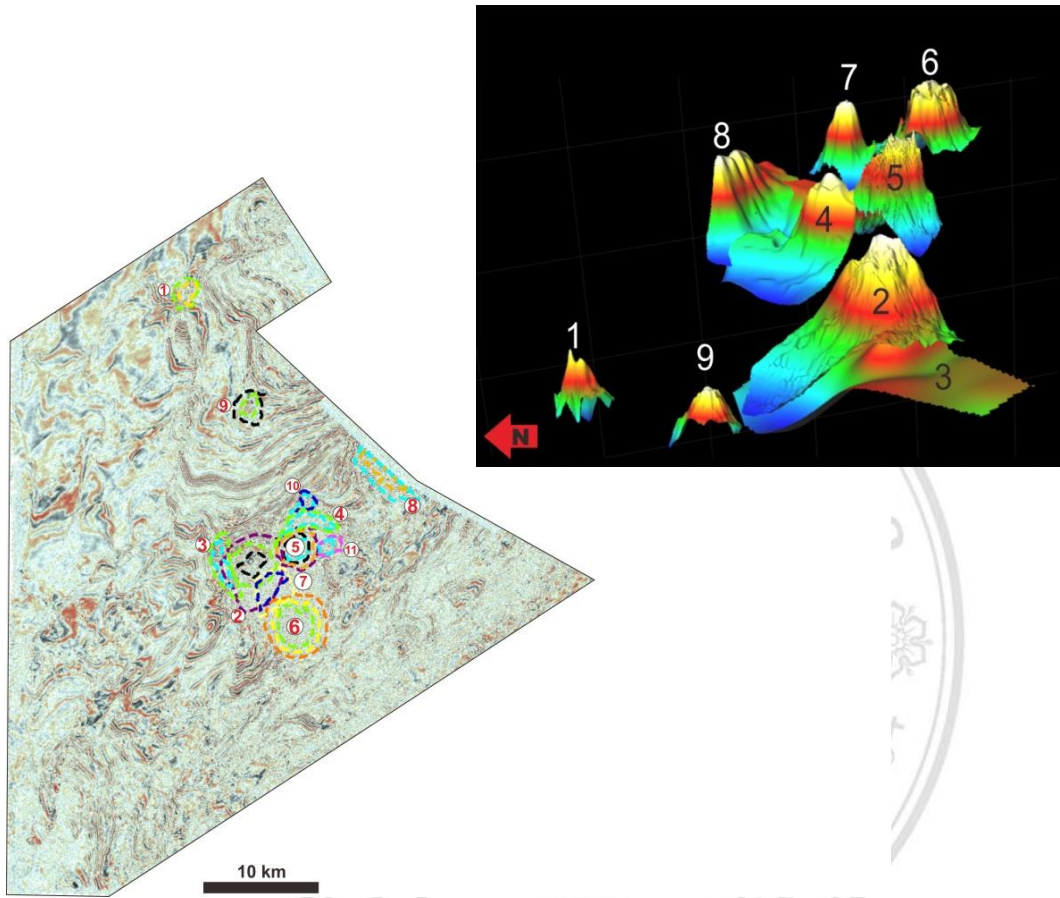


Figure 3. 14 Showing map view and 3 dimensional distribution of the edifices in the study area

ลิขสิทธิ์มหาวิทยาลัยเชียงใหม่
 Copyright© by Chiang Mai University
 All rights reserved

3.5.2.1 Edifice 1

It is the second edifice upon moving away from the north. It has dip values of its flanks ranging from 7-22°. It has average height of 322 m. It possesses the volume of 0.69 km³. It has basal diameter of 2871 m. it is located on IL 4300 and XL 10000. It has a reflection free zone inside and high amplitude reflectors at its flanks. It exhibits truncations with reflectors that lie stratigraphically above it. It sits beneath a fault and has the external form of mound. A seismic section view, growth with time and time structure map are shown in Fig. 3.15 (A, B, and C) respectively.

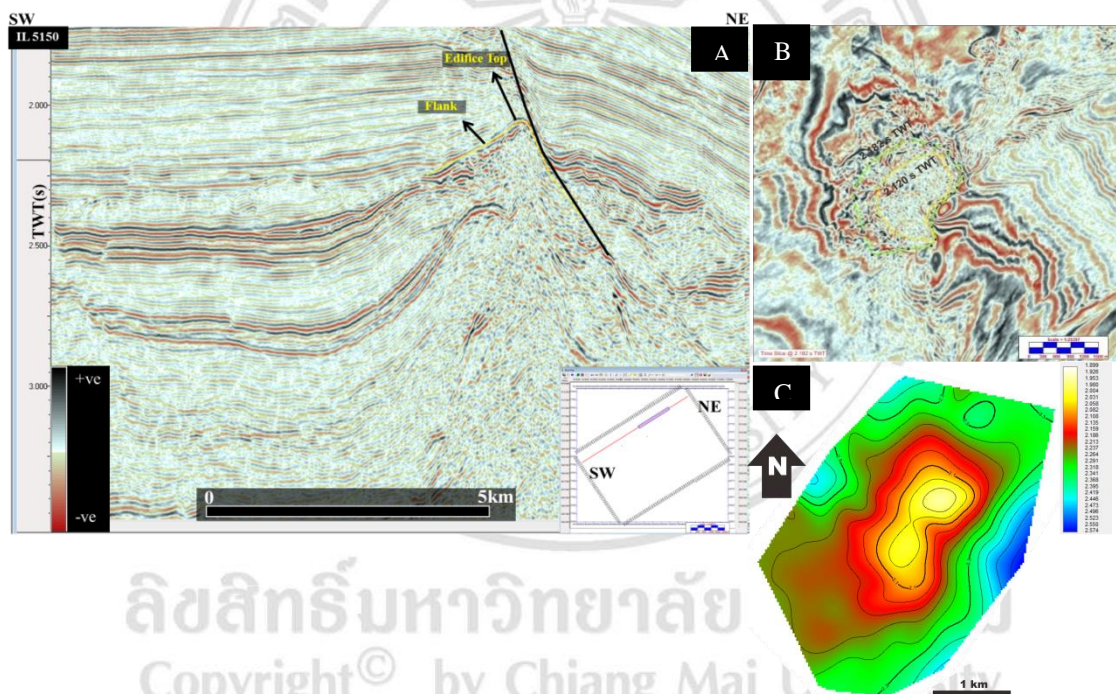


Figure 3.15 A) seismic section view of the edifice 1, B) delineation on time slice, C) time structure map of edifice 1(reference fig. 3.14).

3.5.2.2 Edifice 2

Edifice 2 can be best viewed at XL 8700 and IL 3500. It has basal diameter of 4448.1 m, average height of 312 m. Its dip angles range from 6-12°. It has volume of 4.88 km³. It has gentle top and it sits next to the intrusive body. It has high amplitude reflector at its flank. Chaotic internal reflection

pattern and some medium to high amplitude reflectors are also found. It has gentle top and a depression is found at its top. The SW flank of this edifice is steeply dipping and its NE flank is gently dipping. Its cross-section view, delineation on time slice and time structure map can be seen in Fig. 3.16 (A, B, C) respectively.

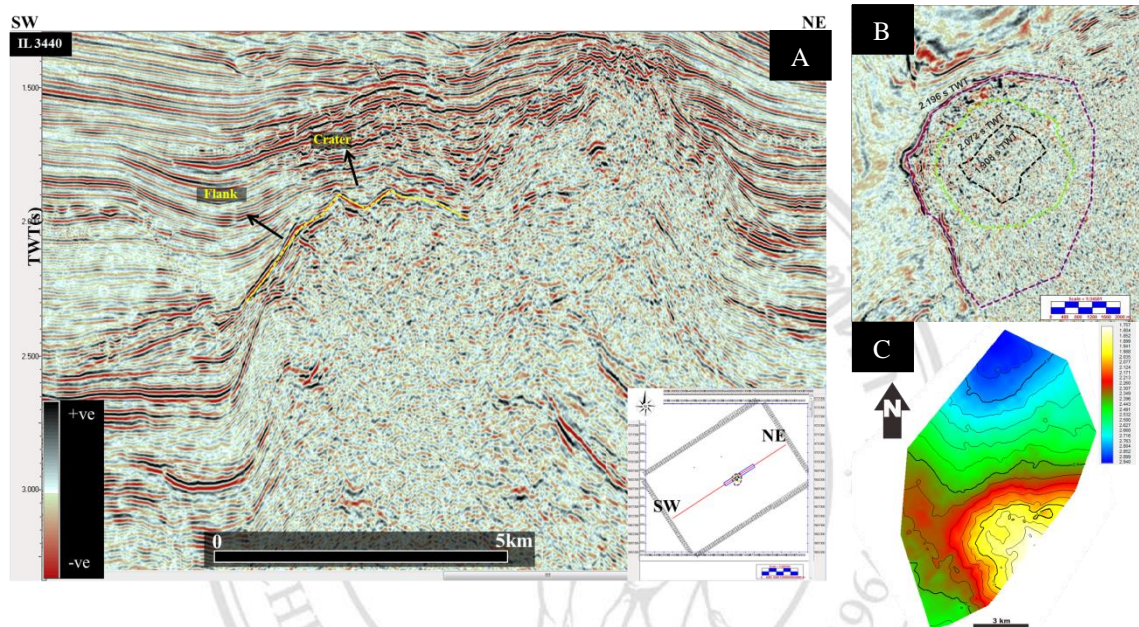


Figure 3.16 A) seismic section view of the edifice 2, B) delineation on time slice, C) time structure map of edifice 2(reference fig. 3.14).

3.5.2.3 Edifice 3

It can be best seen at XL 8700; IL 3650. Dip values of its flanks range from 6—18°. It has basal diameter of 1977m and average height of 212m. It has external form of mound and low amplitude reflectors inside. The reflectors above it have high amplitude and it cross-cuts the reflectors above. It exhibits a very sharp top on some inlines and in some places it has convex upward external form. Its expression is on time slice in Fig. 3.17 (B).

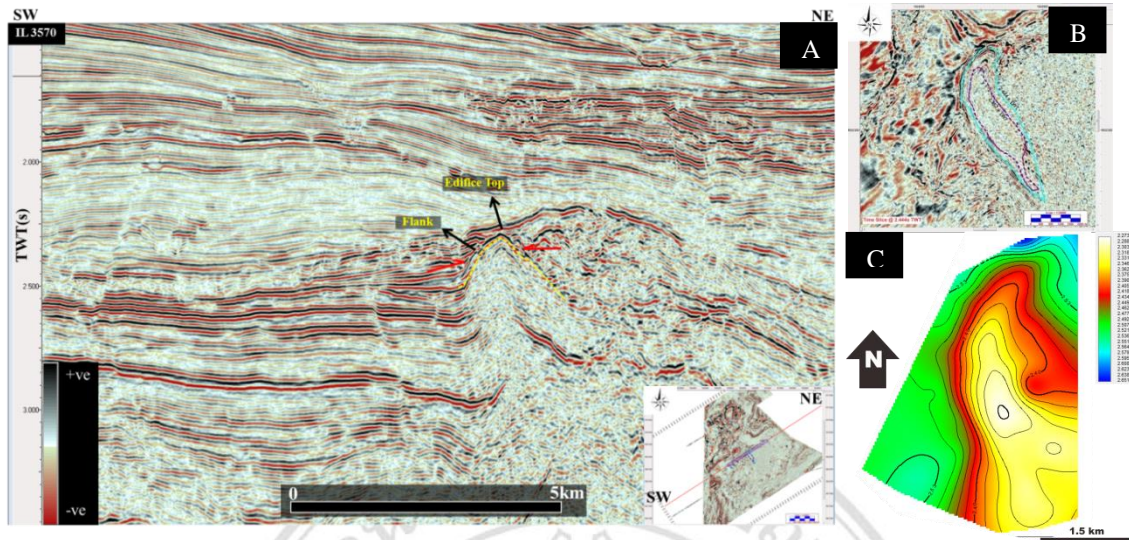


Figure 3.17 A) seismic section view of the edifice 3, B) delineation on time slice, C) time structure map of edifice 3(reference fig. 3.14).

3.5.2.4 Edifice 4

Edifice 4 is preset at XL 9600; IL 3450. It has a chaotic internal reflection pattern. It is located just next to a cone shape intrusive body. It has an external form that is convex upward. The dip values of its flanks range from 9—21°, average height 286 m, and basal diameter 3449 m. It has onlap relationship with overlying reflectors. It has gentle top and it has equal slope on both sides. Its cross-section view, delineation on time slice and time structure map can be seen in Fig. 3.18 (A, B, C) respectively.

ลิขสิทธิ์มหาวิทยาลัยเชียงใหม่
 Copyright© by Chiang Mai University
 All rights reserved

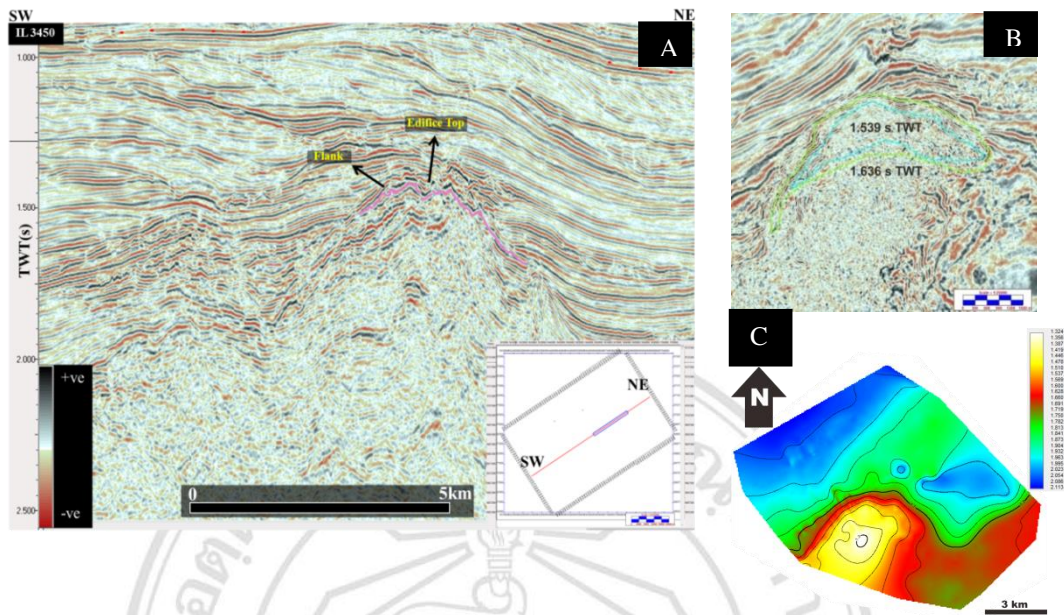


Figure 3.18 A) seismic section view of the edifice 4, B) delineation on time slice, C) time structure map of edifice 4(reference fig. 3.14).

3.5.2.5 Edifice 5

It has dip values of its flanks ranging from 6—16°. Its average height is 430 m; basal diameter is 6094 m and volume of 11.3 km³. It has gentle top dipping towards inside and it has chaotic internal reflection pattern. It has external form of mound. It has parallel dipping reflectors of high amplitude at its flanks. The reflectors are onlapping it from the NE and SW. It can be best viewed at IL 3250. The reflectors of edifice 5 make a cross-cutting relationship with the reflectors lying over it. Its seismic section view, evolution of growth with time and time structure map can be seen in Fig. 3.19 (A, B, C) respectively.

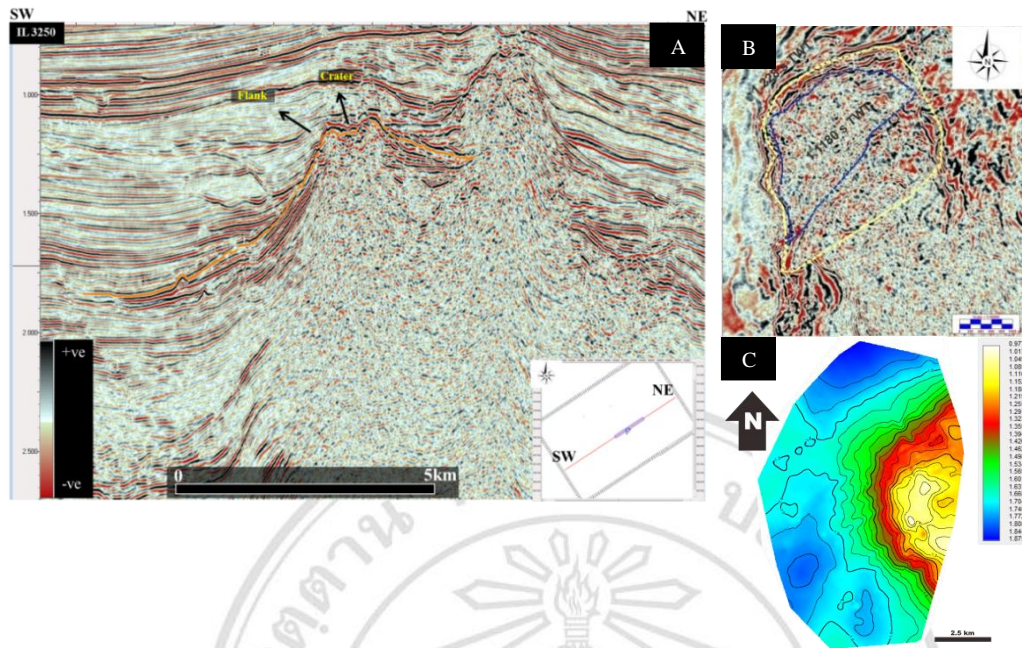


Figure 3.19 A) seismic section view of the edifice 5, B) delineation on time slice, C) time structure map of edifice 5(reference fig. 3.14).

3.5.2.6 Edifice 6

This extrusive body can be best viewed at IL 2850 and XL 8800). Its flanks have dip values ranging from 9—15°. It has a basal diameter of 6732 m, average height of 470 m and volume of 17.2 km³. It has chaotic internal reflection pattern, with parallel dipping reflectors at its flanks of medium to high amplitude. It has a gentle top dipping inwards toward an inferred crater, and the external form of mound, overlying reflections onlap the mound. It has some parallel reflectors inside dipping in the same direction as of its flanks, which become chaotic beneath its top. Its seismic section view, map view in time slice, and time structure map can be seen in Fig. 3.20 (A, B, C) respectively.

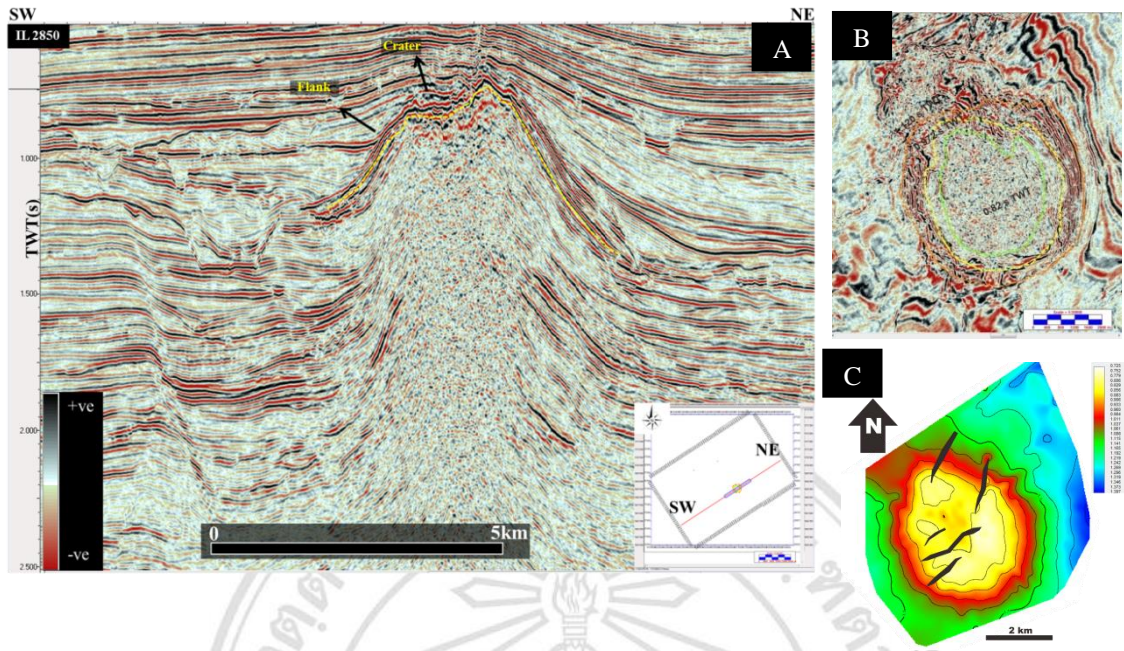


Figure 3.20 A) seismic section view of the edifice 6, B) delineation on time slice, C) time structure map of edifice 6(reference fig. 3.14).

3.5.2.7 Edifice 7

It is located at XL 9400 and IL 3300. It has dip values of its flanks in ranging from 14—20°. It has average height of 454 m, basal diameter of 6732 m and volume of 7.35 km³. It has high amplitude reflectors at its top and chaotic internal reflection pattern. Its flanks onlap on the edifice below. At its SW flank it makes local wedge shape geometry. At its flanks it has parallel to hummocky reflection pattern. It has the external form of mound. Its cross-sectional view, delineation of it with time on map view and time structure map can be seen in Fig. 3.21(A, B, C) respectively.

Copyright © by Chiang Mai University
All rights reserved

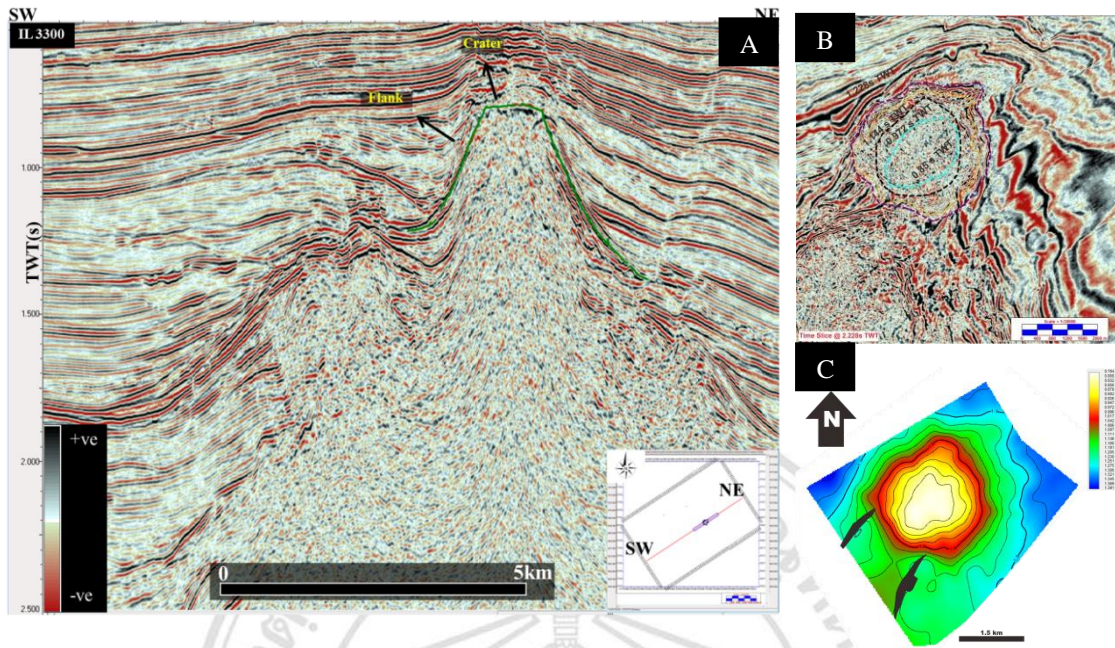


Figure 3.21 A) seismic section view of the edifice 7, B) delineation on time slice, C) time structure map of edifice 7(reference fig. 3.14).

3.5.2.8 Edifice 8

Edifice 8 is present at XL 10900; IL 3500. This edifice has dip values of its flanks in the range of 8—15°, an average height of 298 m, basal diameter of 4130 m and a volume of 3.24 km³. It has parallel to chaotic internal reflection patterns. Its flanks have high amplitude and the overlying reflectors onlap on it. It has been faulted on its top, and has the external form of mound.

ลิขสิทธิ์มหาวิทยาลัยเชียงใหม่
 Copyright© by Chiang Mai University
 All rights reserved

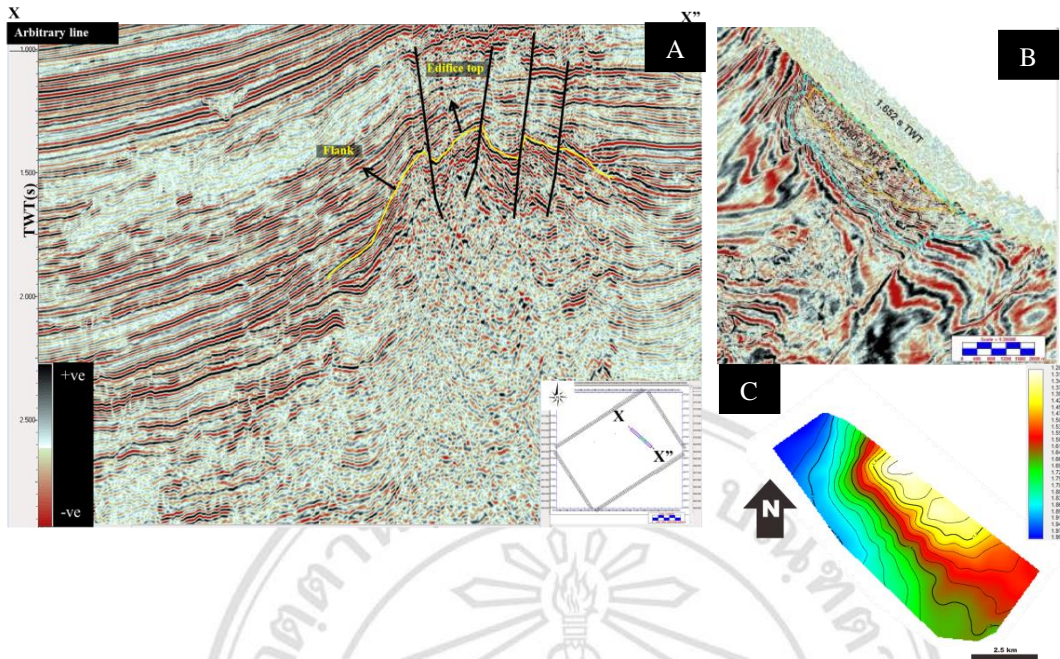


Figure 3.22 A) seismic section view of the edifice 8, B) delineation on time slice, C) time structure map of edifice 8(reference fig. 3.14).

3.5.2.9 Edifice 9

This volcanic edifice has been labelled as 9 (reference Fig. 3.12) has flank dip values that range from 9—21°. Its dip angles were calculated from eight sides which helped to constrain its geometry. Its basal diameter is 3281.1 m; average height is 408 m, and a volume of 1.15 km³. It is located on IL5200 and XL10100. Its cross-sectional view, delineation on time slice and time structure map can be seen in fig 3.13 (A, B, C) respectively.

ลิขสิทธิ์มหาวิทยาลัยเชียงใหม่
Copyright© by Chiang Mai University
All rights reserved

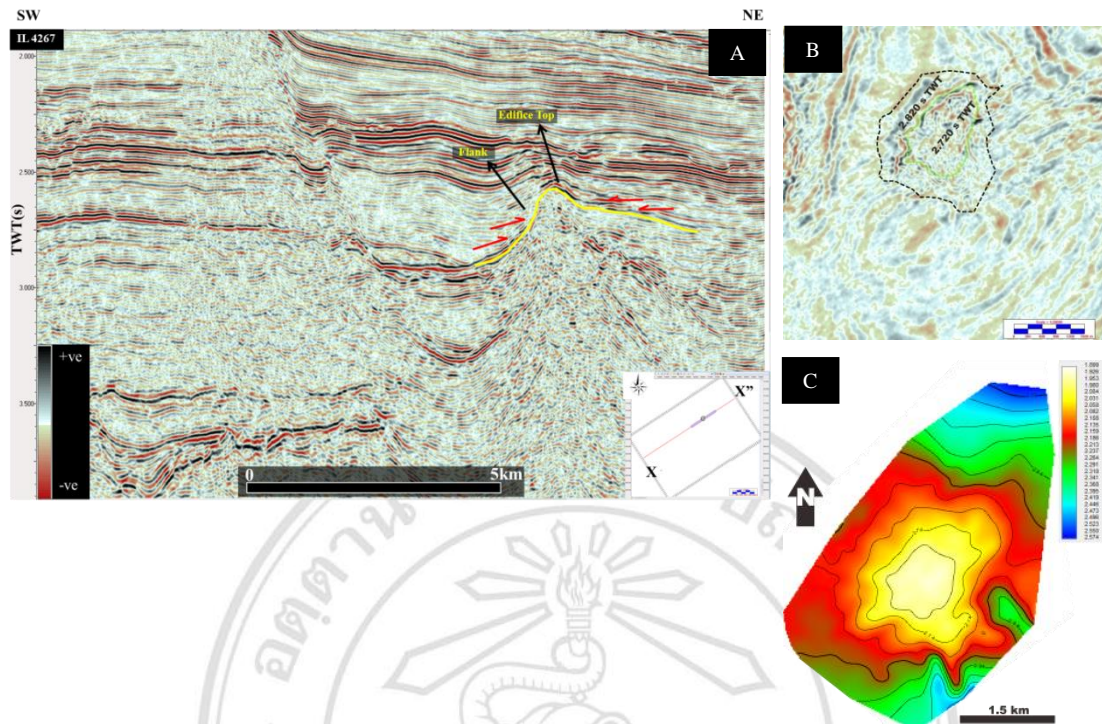


Figure 3.23 A) seismic section view of the edifice 9, B) delineation on time slice, C) time structure map of edifice 9(reference fig. 3.14).

3.5.2.10 Edifice 10

It has flank dip values that range from 8—17°, an average height of 172 m, and a basal diameter of 1448 m and volume of 0.08 km³. It is located at XL 9890; IL 3580. It has chaotic internal reflection pattern and the external form of cone. The dip of the reflectors at its flanks is high and become gentler and eventually flat upon moving away from the intrusion. There is another high amplitude cone-shaped reflector inside it. There is onlap of reflectors on this intrusion. It's seismic section, time slice and time structure map of the edifice is given in Fig. 3.24 A, B and C respectively.

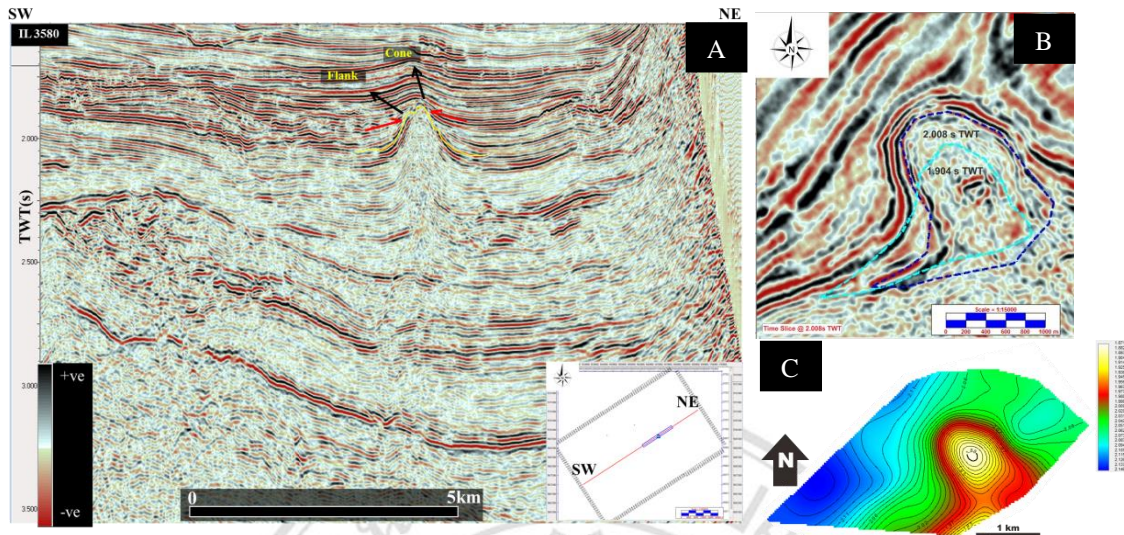


Figure 3.24 A) seismic section view of the edifice 10, B) delineation on time slice, C) time structure map of edifice 10 (reference fig. 3.14).

3.5.2.11 Edifice 11

Edifice 11 is located around IL 3150 and XL 9800. It has dip values of its flanks ranging from 4-9° and the external form of a mound. It has average height of 149 m a volume 0.89 km³ and basal diameter of 4793 m, with low amplitude internal reflections. It exhibits onlap of overlying reflections. It has no data zone on its NW side. It has parallel dipping reflectors inside making similar shape with the edifice 11.

ลิขสิทธิ์มหาวิทยาลัยเชียงใหม่
 Copyright© by Chiang Mai University
 All rights reserved

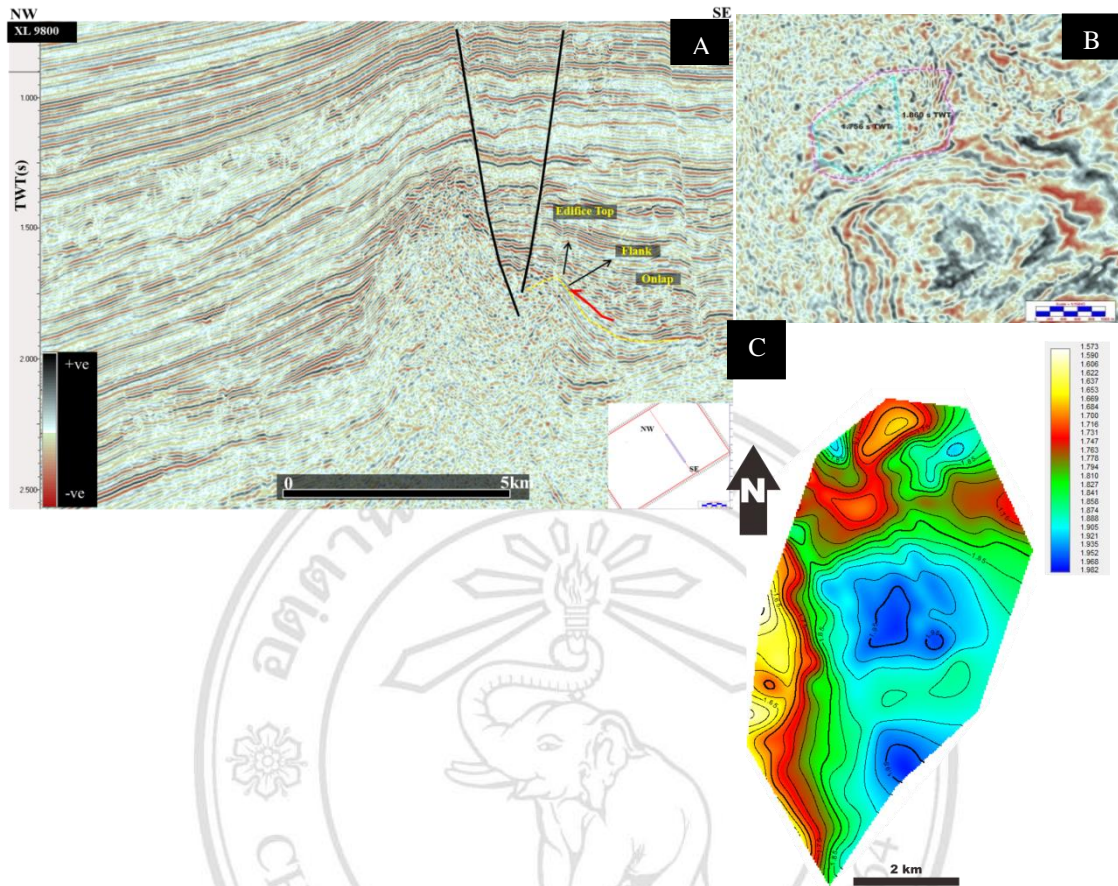


Figure 3.25 A) seismic section view of the edifice 11, B) delineation on time slice, C) time structure map of edifice 11(reference fig. 3.14).

ลิขสิทธิ์มหาวิทยาลัยเชียงใหม่
 Copyright© by Chiang Mai University
 All rights reserved

3.6 Quantification of edifice shape

Measurements of basic edifice shape values were made from the seismic data (Figs. 3.26 and 3.27) and their results were compared with the measurements of the onshore volcanoes located on Taranaki peninsula near the study area (Fig. 3.28).

3.6.1 A (Volume vs. Basal diameter)

Graph (A) Fig. 3.26 shows that with the increase on basal diameter the volume also increases constantly except the one anomaly located near the y-axis. Most of the values lie in the range of 0—2 km³ volume and approximately 1—4 km of basal diameter (Fig. 3.26 A).

3.6.2 B (Average height vs. Basal diameter)

Graph B Fig.3.26 shows that there is a constant relationship between basal diameter and height. There is a continuous increase in the trend and maximum basal diameter shows maximum height (Fig. 3.26 B).

3.6.3 C (Average height vs. Average angle of the flanks)

Graph C Fig.3.26 shows that most of the values lie in range of 0.2—0 km of average height and that most values of the flank dips are in the range of 6—20°(Fig. 3.26 C).

3.6.4 D (Slope angle vs. Azimuth)

Graph D Fig.3.27 shows the random values of slope angle plotted against azimuth. At each point there is a constant trend of the slope angles vs. azimuth (Fig. 3.27 D).

3.6.5 E (Average height vs. Volume)

Graph E fig.3.27 shows that as the height increase the volume also increases and there is a cluster of values located near the axis and three values show fairly same trend (Fig. 3.27 E).

3.6.6 F (Average height vs. Volume)

Graph F, Fig.3.27 shows scattered values of average basal diameter against the average angle of the flanks. There is a high and low trend upon moving from 0 to the right and 0 to up (Fig. 3.27 F).

3.7 Quantification results of the onshore volcanoes

3.7.1 Azimuth vs. Dip of the flanks

It shows random values of the azimuth plotted against the dip of the flanks

3.7.2 Height vs. Basal diameter

It shows a constant increase in the values for three different onshore volcanoes. Volanco-1 shows the height values of basal diameter and height (Fig. 2.28).

3.7.3 Height vs. dip of the flanks

It shows cluster of the values near the axis of the graphs and one group of values away from the axis (Fig. 2.28).

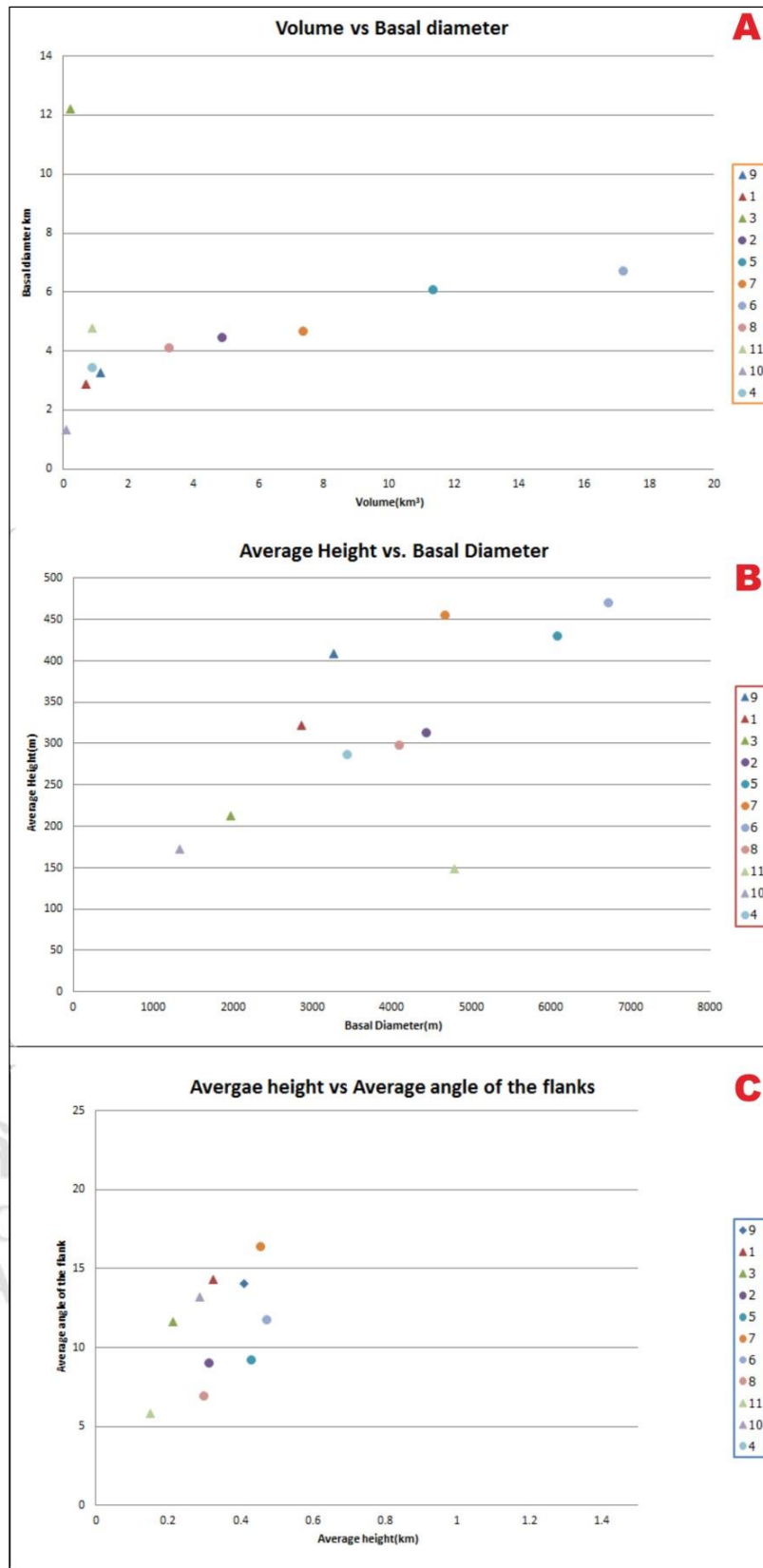


Figure 3.26 Graphs showing the quantification results (A, B, C).

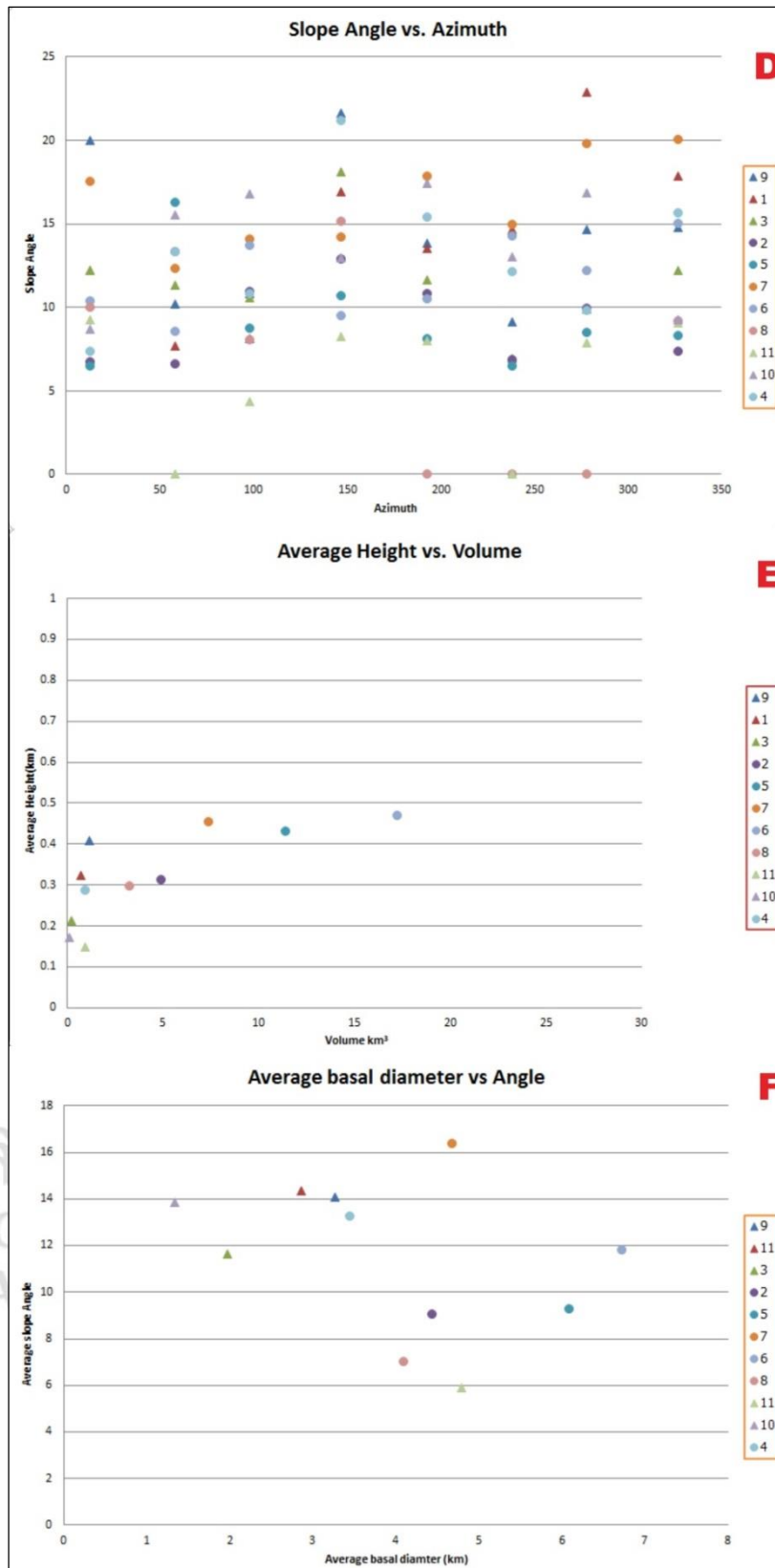


Figure 3.27 Graphs showing the quantification results (D, E, F).

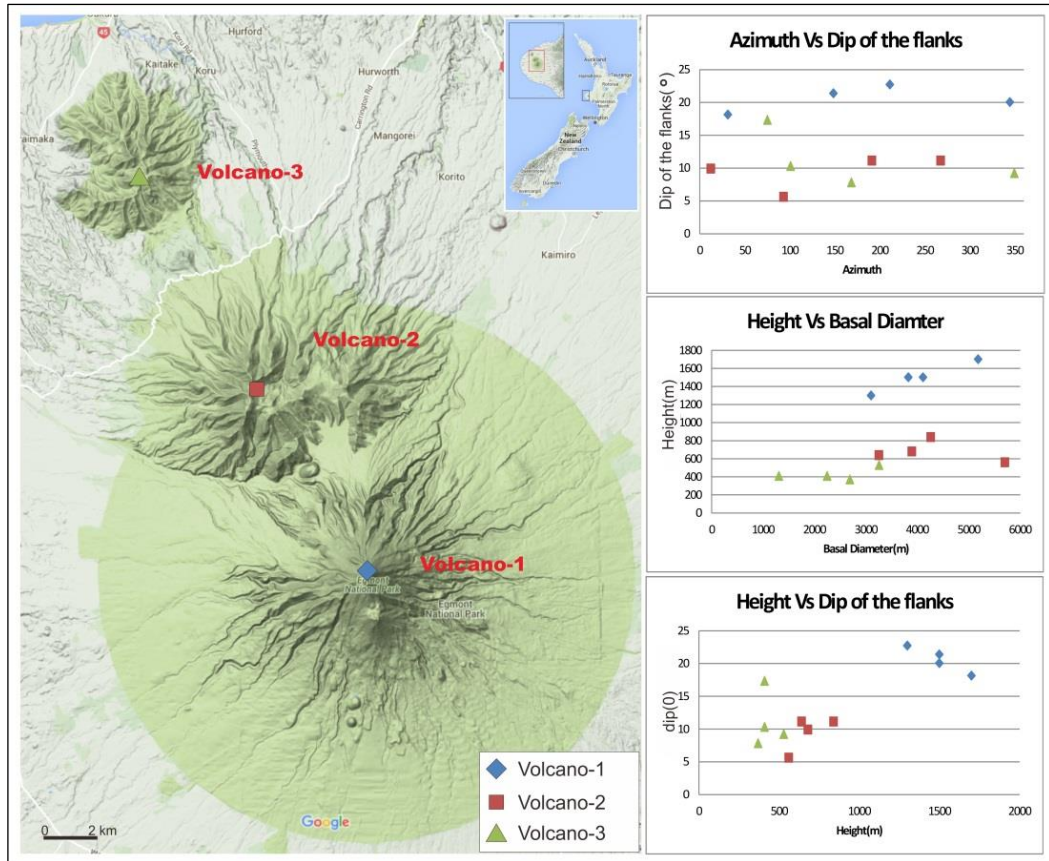


Figure 3.28 showing the quantification results of the onshore volcanoes located on the Taranaki peninsula.

3.8 Well data analysis

The well is located within the study area. The well location is given in (Fig. 2.1). The well was drilled vertically to a local depth of 3055m; 3038m subsea. The water depth at the location was 132m. GR log shows alternations of sand and shale with bell shape log response, coarsening upward and fining upward. A thick unit of volcanic tuff was found in Mohakatino formation which shows similar trend to shale in the GR log (Fig. 3.29).

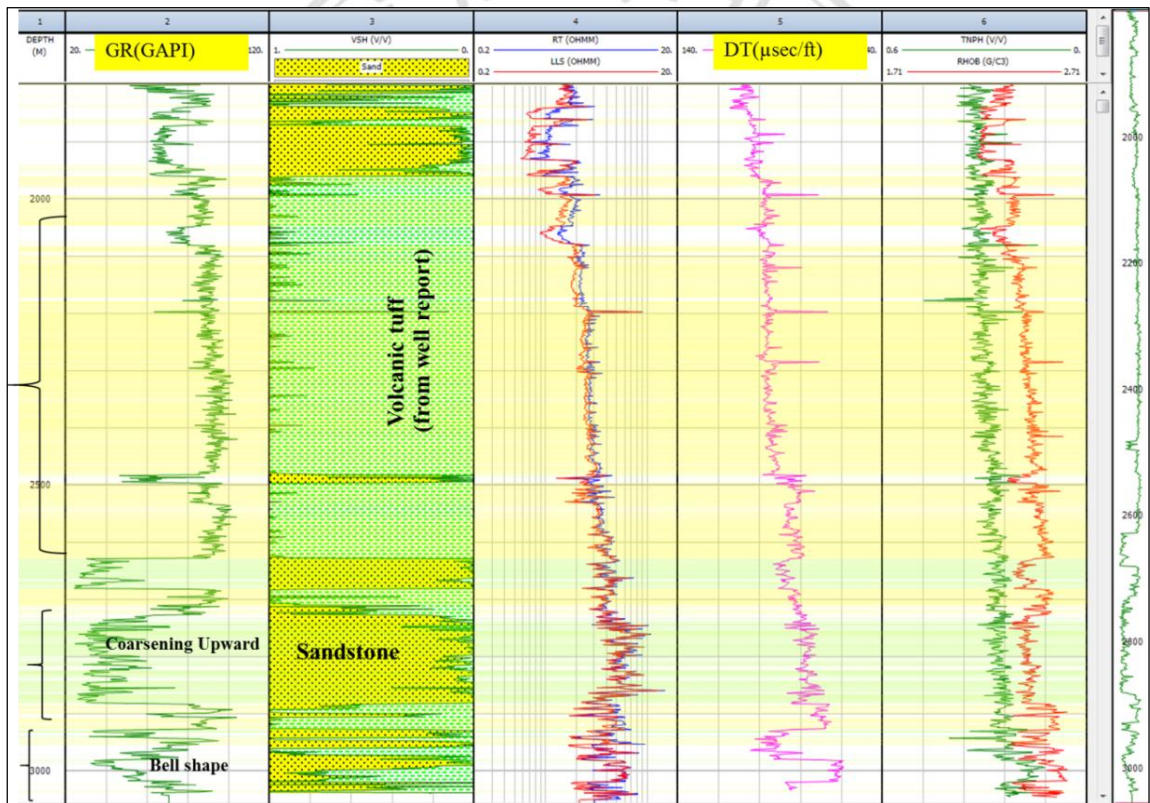


Figure 3.29 well log plots for Arawa-1 showing the distribution of shale, sand and tuff.

3.8.1 Cross-plot between DT vs. Depth

Cross-plot for DT vs. depth shows normal trend with increasing depth except three DT anomalies which was interpreted as gas peaks in well report Fig. 3.30.

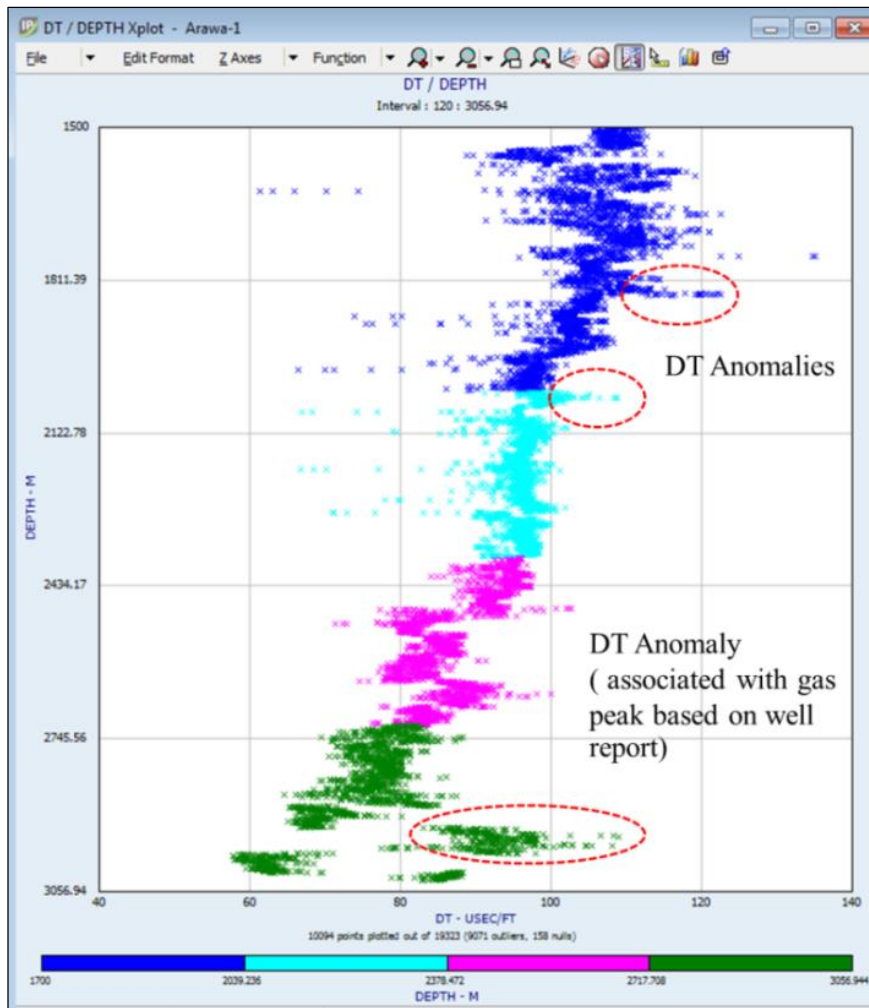


Figure 3.30 Cross plot between DT vs. Depth showing the compaction trend.

3.8.2 Cross-plot between RHOB vs. GR and depth

A cross-plot between GR vs. RHOB with depth on Z-axis shows the distribution of sand, shale and tuff. Tuff shows similar behavior in GR log as shale and its depth range was obtained from well report and was highlighted on the cross-plot (Fig. 3.31).

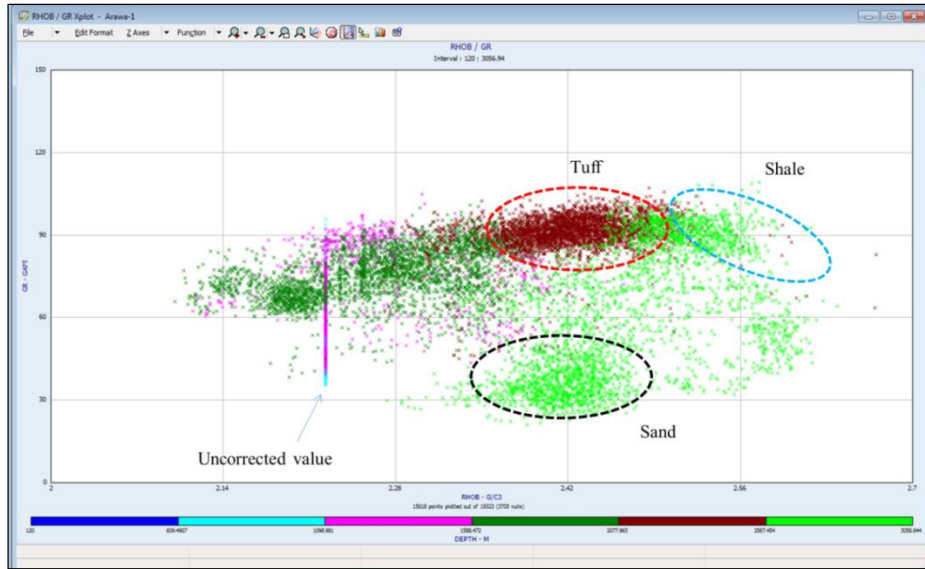


Figure 3.31 Showing cross-plot between vs. RHOB with depth on Z-axis showing the distribution of sand, shale and tuff

3.8.3 Time-depth chart

Time depth chart was used from the well report and was used to tie with the seismic. T-D chart graph (Fig. 3.32).

T-D Chart for Arawa-1 well

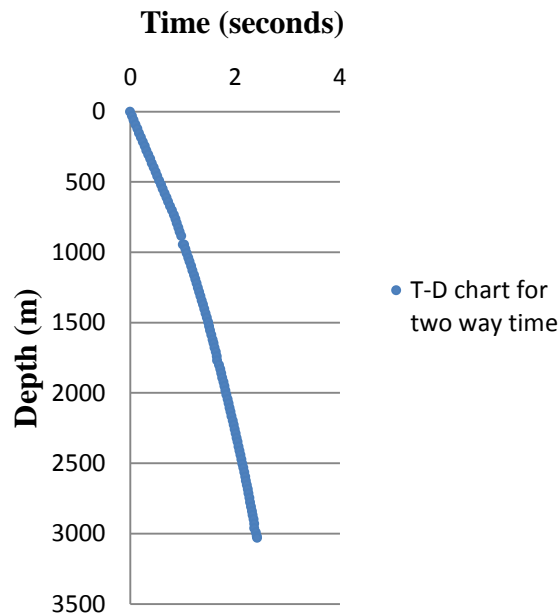


Figure 3.32 Time -Depth chart for Arawa-1 well based on well report.

3.9 Seismic stratigraphic and volcano stratigraphic analysis

3.9.1 Edifice 1

Edifice-1 shows cross-cutting of the reflectors it is intruding. It shows local erosional surface and then onlap of the reflectors on that erosional surface. It shows the local wedge shape geometry along the fault. Downlap of reflections occurs in the structural low (Fig. 3.32) Time slice at 2.404 s TWT shows the channels. It has meandering channel which is going from east to west. One channel direction is from north to south passing near the flank of the edifice (Fig. 3.33).

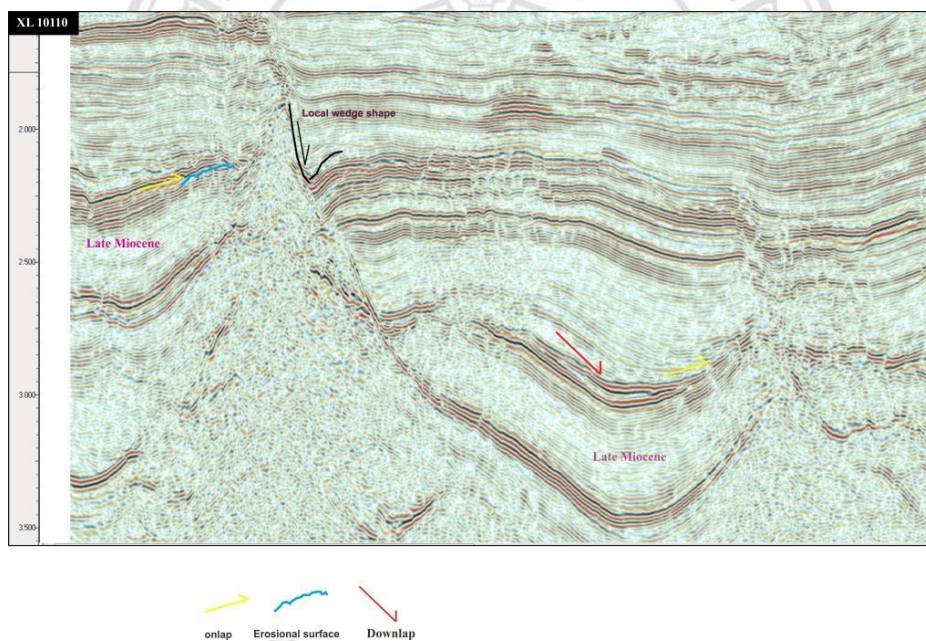


Figure 3.33 A cross-section showing the local wedge shape geometry along the fault.

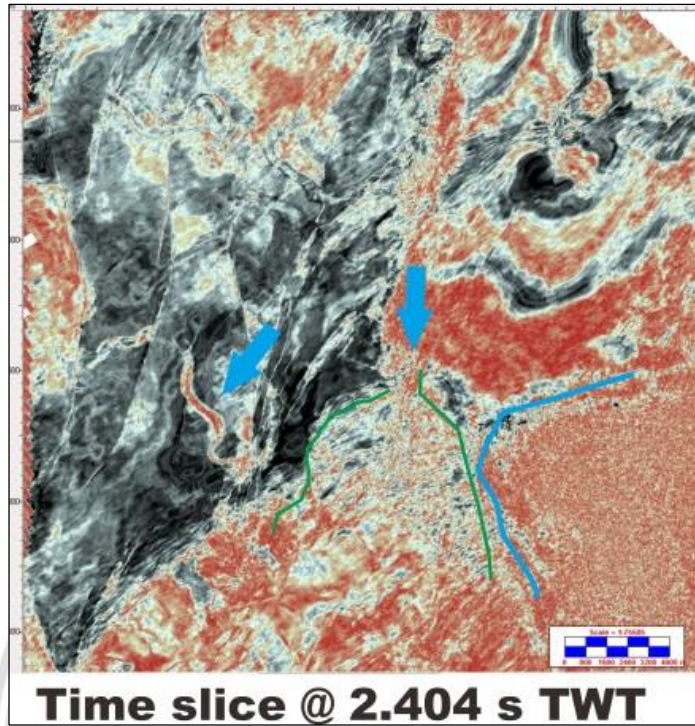


Figure 3.34 Time slice at 2.404 s TWT overlaid with RMS shows direction of channels.

ลิขสิทธิ์มหาวิทยาลัยเชียงใหม่
Copyright© by Chiang Mai University
All rights reserved

3.9.1.1 Edifice 1

Time slice at 2.183 shows local radial drainage pattern going away from the edifice 1. The channel direction is dominantly towards NW (Fig. 3.35).

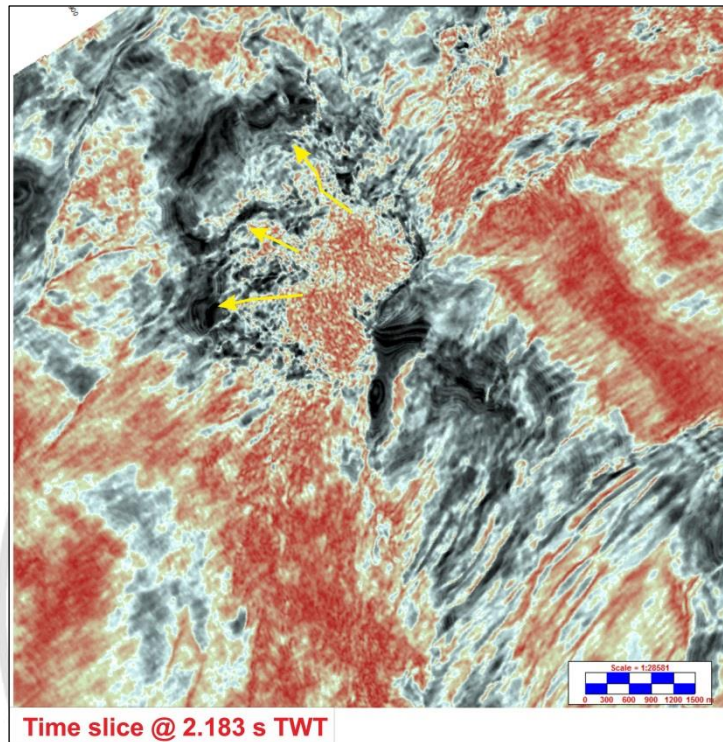


Figure 3.35 showing radial drainage pattern in time slice at 2.183 s TWT overlaid with RMS

3.9.2 Edifice 2

ลิขสิทธิ์มหาวิทยาลัยเชียงใหม่
Copyright© by Chiang Mai University
All rights reserved

Edifice 2 shows onlap of the strata at its flanks and a local depression at its top. It has high amplitude reflector at its top (Fig. 3.36).

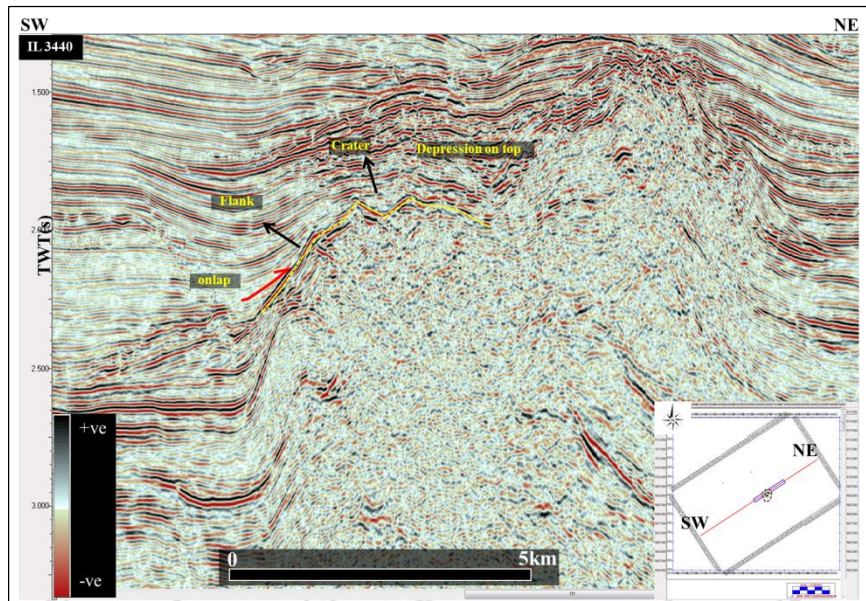


Figure 3.36 showing the onlap relationship of the edifice 2.

3.9.3 Edifice 3

A cross-section through Edifice-3 shows the constant thickness of the overlying package on both sides of the flanks and local erosional surface and onlap of the reflectors onto the erosional surface (Fig. 3.37).



Figure 3.37 intrusive body showing the constant thickness on both sides and thinning on top

3.9.4 Edifice 4

It shows the onlap of reflectors at its SW and NE flanks. The unit above this edifice has constant thickness (Fig. 3.38)

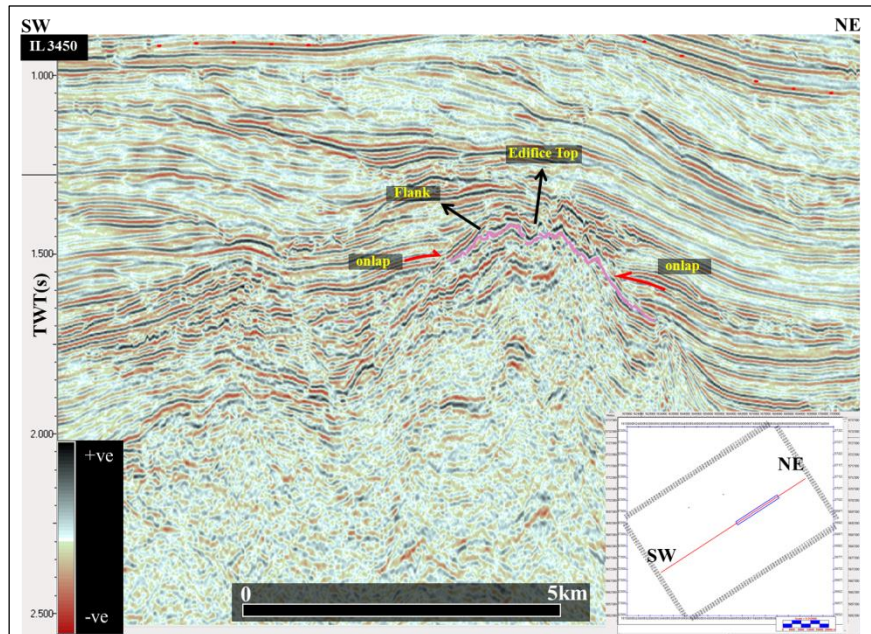


Figure 3.38 showing the onlap relationship of the edifice 4

3.9.5 Edifice 5

Figure 3.39 shows the onlap of the reflectors at its flanks and downlap at its NE flank. It has local depression at its top.

ลิขสิทธิ์มหาวิทยาลัยเชียงใหม่
Copyright© by Chiang Mai University
All rights reserved

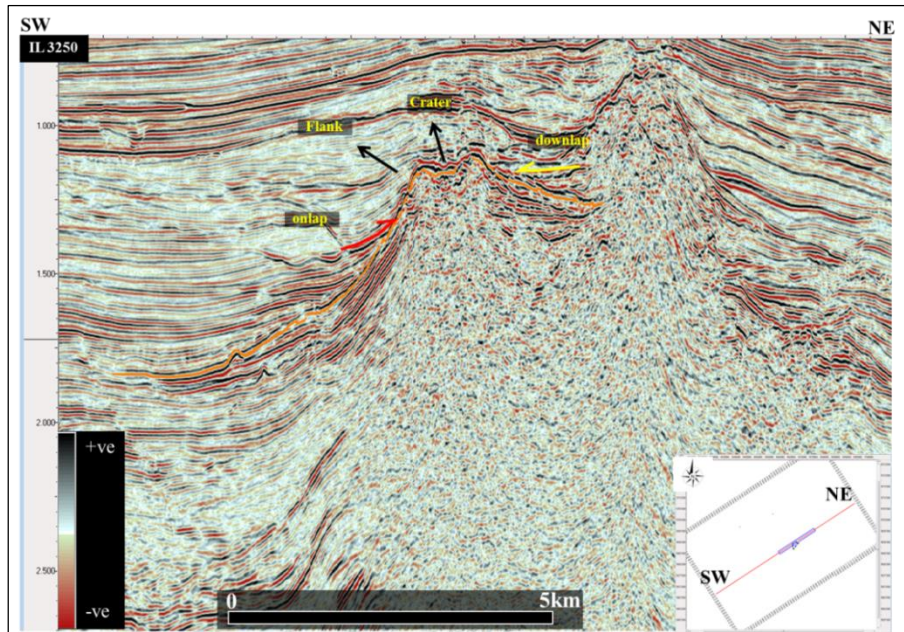


Figure 3.39 seismic stratigraphic relationship of the edifice 5

3.9.6 Edifice 6

It has onlap of the reflectors at its SW flank and a downlap on the reflectors away from the edifice at the NE flank. Time slice overlaid with the RMS shows the high amplitude reflectors that decrease in thickness and amplitude passing away from the edifice (Fig. 3.40).

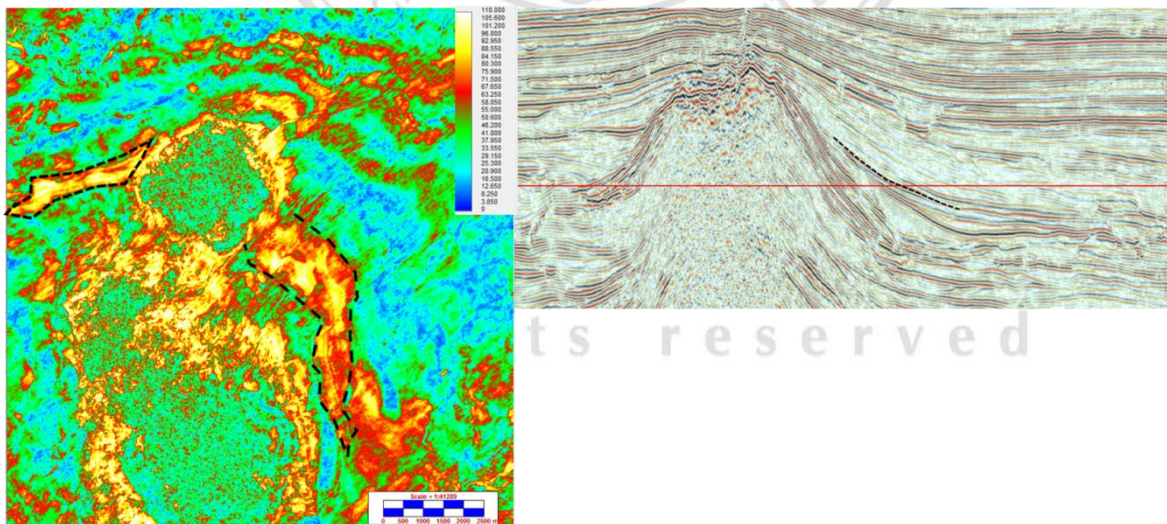


Figure 3.40 RMS time slice at 1.164 s TWT.

3.9.7 Edifice 9

IL 4200 shows the onlap and down lap of the reflectors on located on top of edifice 9. On the SW flank of the edifice a local depression is seen (Fig. 3.41).

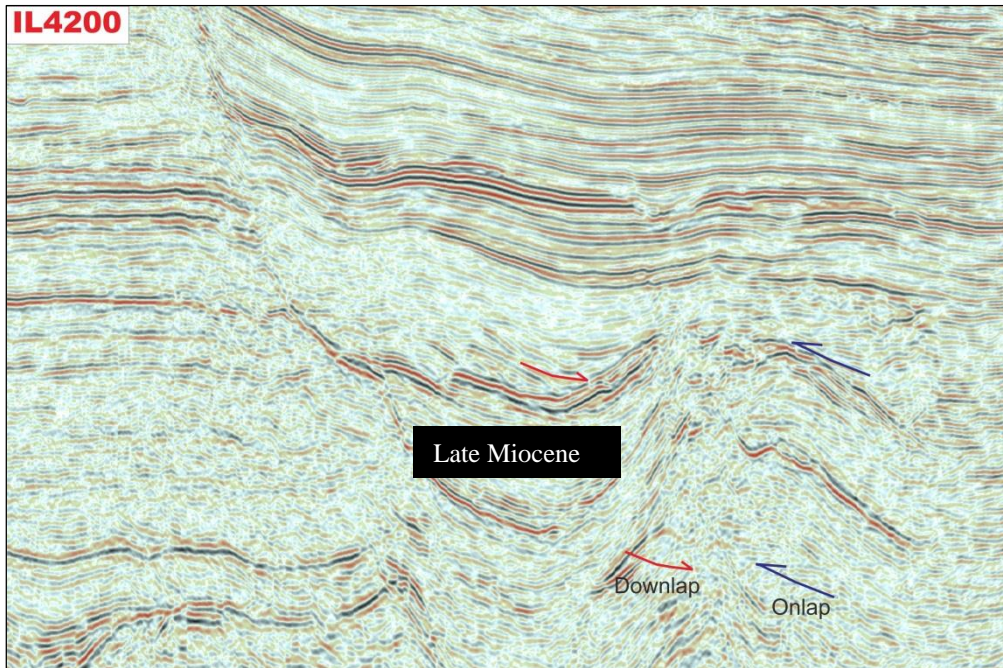


Figure 3.41 IL 4200 showing the onlap and downlap of the reflectors

3.9.8 Horizon slice at H-4 Horizon

Horizon slice overlaid with the RMS shows the radial drainage pattern going away from the edifices. Radial drainage pattern is seen along the edifice 9 (Fig. 3.42).

ลิขสิทธิ์มหาวิทยาลัยเชียงใหม่
 Copyright© by Chiang Mai University
 All rights reserved

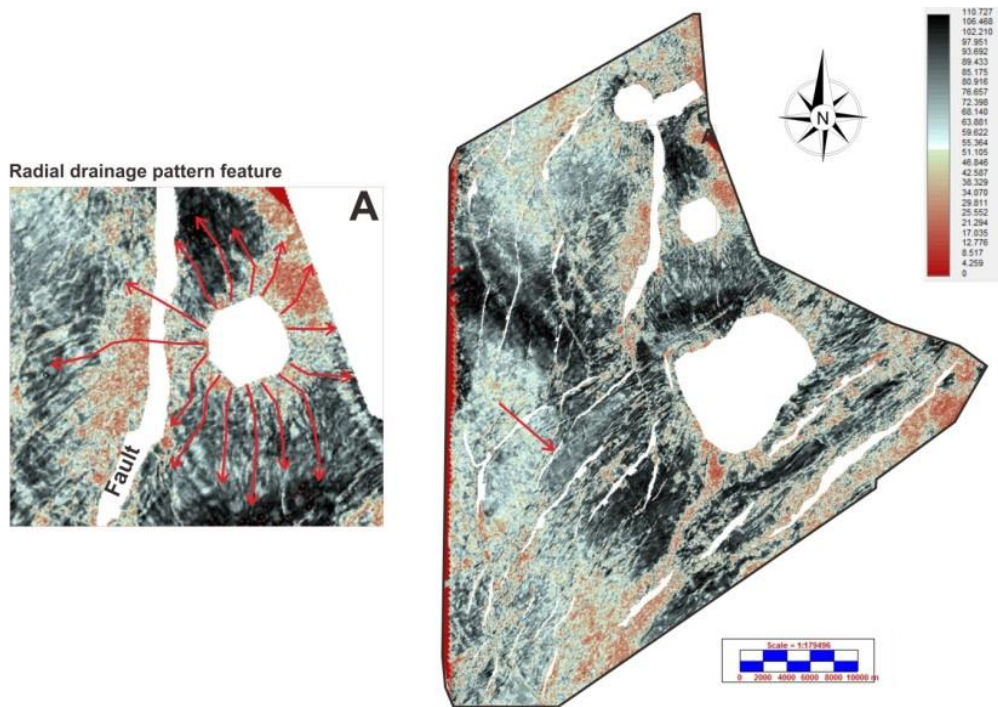


Figure 3.42 Extracted RMS amplitudes on H-4 horizon

3.9.9 Horizon slice along phantom horizon created 250 ms above H-4

Horizon slice created along phantom horizon created 250 ms above the H-4 horizon shows the channel being deflected by the fault and channel is dying out at another fault (Fig. 3.43).

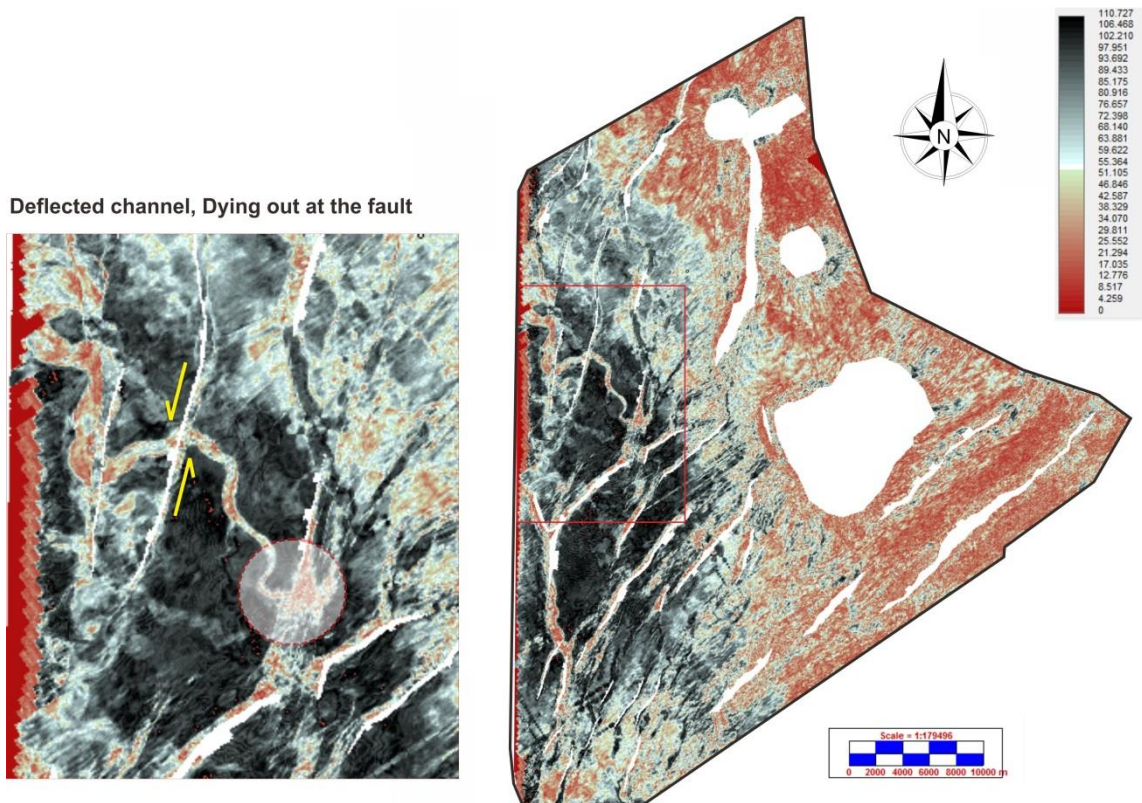


Figure 3.43 phantom horizon created 250 ms the H-4 horizon

3.9.10 Horizon slice along the H-8

Horizon slice created along H-8 horizon overlaid with RMS shows patchy surfaces and some sinuous channels going in different directions (Fig.3.44).

ลิขสิทธิ์มหาวิทยาลัยเชียงใหม่
 Copyright© by Chiang Mai University
 All rights reserved

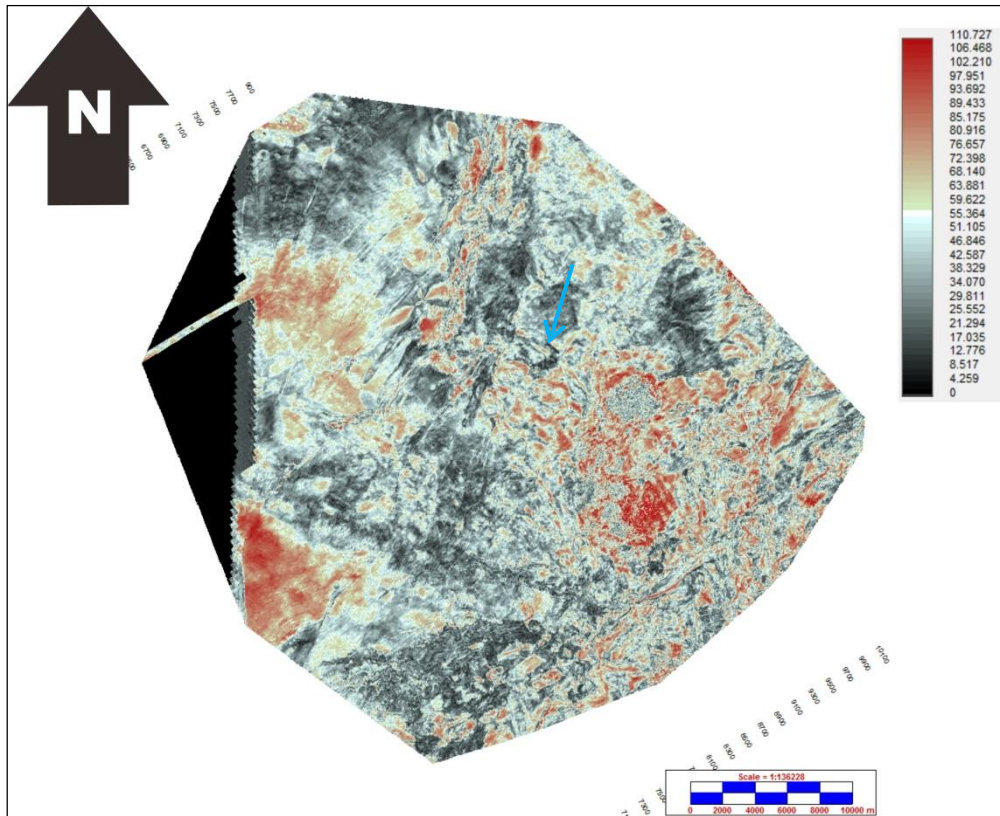


Figure 3.44 H-8 horizon with RMS amplitude extraction.

3.9.11 Horizon slice generated along additional horizon A(was not incorporated into maker horizon):

Horizon slice overlaid RMS along horizon A shows the meandering channel trending NE to SW and some other channels trending from east to west (Fig. 3.45).

ลิขสิทธิ์มหาวิทยาลัยเชียงใหม่
Copyright© by Chiang Mai University
All rights reserved

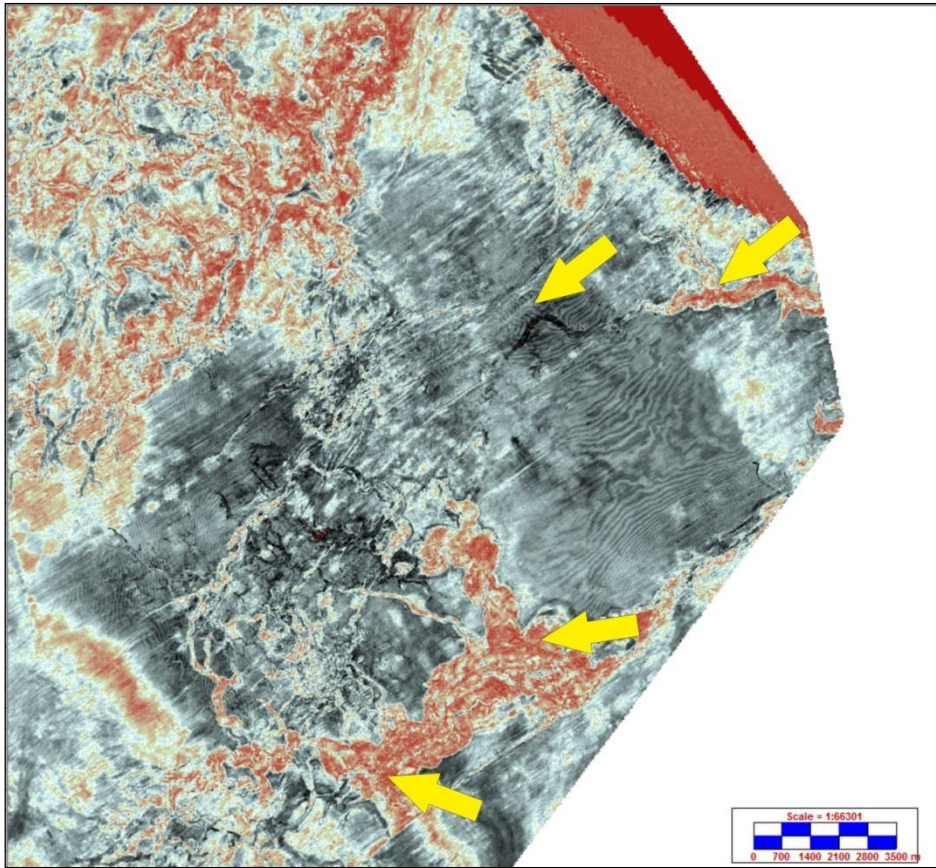


Figure 3.45 RMS extraction along the Horizon A

ลิขสิทธิ์มหาวิทยาลัยเชียงใหม่
Copyright© by Chiang Mai University
All rights reserved